Mohamed Khider University of Biskra
Faculty of Science and Technology
Department of Electrical Engineering

MASTER'S THESIS

Science and Technology
Electrotechnics
Electrical Networks

Réf. : Enter the document reference

Presented and defended by:
BEN ABBAS Khalil and BEN AROUS Amor

On: Tuesday, June 3, 2025

Methods for estimating the state of charge of a battery.

Jury :

Dr.	CHAROUF Omar	Pr	University of Biskra	President
Dr.	MOUSSI Ammar	Pr	University of Biskra	Examiner
Dr.	TIAR Mourad	MCA	University of Biskra	Supervisor

CLASS OF 2024 / 2025

Mohamed Khider University of Biskra
Faculty of Science and Technology
Department of Electrical Engineering

MASTER'S THESIS

Science and Technology
Electrotechnics
Electrical Networks

Réf. : Enter the document reference

Methods for estimating the state of charge of a battery.

On: Tuesday, June 3, 2025

Presented by:

BEN ABBAS Khalil
BEN AROUS Amor

Favorable opinion of the supervisor:

TIAR Mourad

Favorable opinion of the Jury President:

CHAROUF Omar

Seal and signature

Gratitude and Appreciation

Acknowledgements

First and foremost, we would like to express our sincere gratitude to Allah Almighty, who granted us strength, patience, and perseverance throughout our academic journey.

We would also like to extend our deep appreciation to ***Professor BETKA Achour*** *and* ***Dr. TIAR Mourad****. The latter, in particular, contributed greatly with valuable efforts and guidance that had a significant and meaningful impact on the quality of this research. We are also thankful to the members of the defense committee for their time, evaluations, and constructive feedback.*

Our heartfelt thanks go to all the professors and staff of the Department of Electrical Engineering at ***Mohamed Khider University of Biskra****, whose knowledge and dedication have profoundly shaped our academic experience over the years.*

We would like to express special gratitude to our families, especially our parents, for their unconditional love, encouragement, and sacrifices. Their constant support has been a great source of strength throughout our studies.

Finally, we thank all our colleagues, friends, and everyone who contributed directly or indirectly to the successful completion of this work.

Thank you all.

Dedication

Dedication

We dedicate this work to:

Our dear parents, for their unconditional love, prayers, patience, and sacrifices throughout our academic journey.

To our brothers and sisters, for their moral support and constant encouragement.

To our loyal friends, companions throughout these university years, for the unforgettable moments, collaboration, and support.

And to everyone who, directly or indirectly, contributed to the completion of this modest work.

With all our gratitude and respect.

BEN ABBAS Khalil

BEN AROUS Amor

Abstract

With the growing integration of renewable energy sources and the need for more efficient energy storage, this thesis explores various energy storage technologies, with a particular focus on batteries in photovoltaic (PV) applications. The work begins with a comprehensive review of different storage elements, including lead-acid batteries, AGM batteries, lithium-ion batteries, ultracapacitors, and inertial flywheels, highlighting their characteristics, advantages, and drawbacks.

A detailed modeling of the solar battery is then presented, featuring equivalent electrical models such as the Thevenin model and the hysteresis-based model. Key battery indicators such as State of Charge (SOC), State of Health (SOH), and Depth of Discharge (DOD) are defined, along with a discussion of the main techniques used to estimate SOC.

The final part of the thesis focuses on practical methods for SOC estimation. A traditional Coulomb counting algorithm is implemented, followed by an enhancement using an adaptive law to correct its limitations. A Kalman filter-based approach is also applied, and the different methods are compared through simulation to evaluate their accuracy and responsiveness. The results confirm the effectiveness of each method and their potential for integration into real-time energy management systems.

This thesis contributes to the development of intelligent battery management systems and supports the advancement of reliable and efficient renewable energy storage solutions.

Résumé

Avec l'intégration croissante des sources d'énergie renouvelable et la nécessité d'un stockage d'énergie plus efficace, ce mémoire explore différentes technologies de stockage, en mettant particulièrement l'accent sur les batteries utilisées dans les applications photovoltaïques (PV). Le travail commence par une revue complète des différents éléments de stockage, y compris les batteries au plomb, les batteries AGM, les batteries lithium-ion, les supercondensateurs et les volants d'inertie, en mettant en évidence leurs caractéristiques, avantages et inconvénients.

Une modélisation détaillée de la batterie solaire est ensuite présentée, à travers différents modèles électriques équivalents tels que le modèle de Thévenin et le modèle basé sur l'hystérésis. Les indicateurs clés des batteries, tels que l'état de charge (SOC), l'état de santé (SOH) et la profondeur de décharge (DOD), sont définis, accompagnés d'une discussion sur les principales techniques utilisées pour estimer le SOC.

La dernière partie du mémoire se concentre sur des méthodes pratiques d'estimation du SOC. Une méthode de comptage de Coulomb classique est d'abord implémentée, suivie d'une amélioration via une loi adaptative pour corriger ses limites. Une approche basée sur le filtre de Kalman est également appliquée. Ces différentes méthodes sont comparées à travers des simulations afin d'évaluer leur précision et leur réactivité. Les résultats confirment l'efficacité de chaque méthode et leur potentiel d'intégration dans des systèmes de gestion d'énergie en temps réel.

Ce travail contribue au développement de systèmes intelligents de gestion de batteries et soutient l'évolution de solutions de stockage d'énergie renouvelable fiables et efficaces.

ملخص

مع التوسع المتزايد في اعتماد مصادر الطاقة المتجددة والحاجة إلى تخزين الطاقة ، تستكشف هذه المذكرة مختلف تقنيات تخزين الطاقة، مع تركيز خاص على البطاريات في تطبيقات الأنظمة الكهروضوئية (PV).يبدأ العمل بمراجعة شاملة لمكونات التخزين المختلفة، بما في ذلك بطاريات الرصاص الحمضية، بطاريات AGM، بطاريات الليثيوم، المكثفات الفائقة، وعجلات القصور الذاتي، مع إبراز خصائص كل منها، مزاياها وعيوبها.

يتم بعد ذلك تقديم نمذجة مفصلة للبطارية الشمسية، من خلال استعراض نماذج كهربائية مكافئة مثل نموذج ثيفنين والنموذج القائم على الهيسترة .كما يتم تعريف مؤشرات البطارية الأساسية مثل حالة الشحن(SOC) ، حالة الصحة(SOH) ، وعمق التفريغ(DOD) ، إلى جانب مناقشة أهم التقنيات المستخدمة في تقدير حالة الشحن.

يركز الجزء الأخير من العمل على تطبيق طرق عملية لتقدير حالة الشحن .حيث يتم تنفيذ خوارزمية العد الكولومبي التقليدية، متبوعةً بتحسين باستخدام قانون تكيفي لتصحيح أوجه القصور .كما تم تطبيق نهج يعتمد على مرشح كالمان، وتمت مقارنة الطرق المختلفة من خلال المحاكاة لتقييم دقتها واستجابتها . وأكدت النتائج فعالية كل طريقة وإمكانية دمجها في أنظمة إدارة الطاقة في الوقت الحقيقي.

تُسهم هذه المذكرة في تطوير أنظمة إدارة البطاريات الذكية، وتدعم تقدم حلول تخزين الطاقة المتجددة الموثوقة والفعّالة.

Table of Contents

Abstract……..….
IV

Table of Contents……...……. *IV*

List of Figures …….……. *IV*

List of Tables…….……...…… *IV*

Symbols and notations……...……*IV*

General Introduction……*IV*

General Conclusion …….…….*IV*

References……..……...*IV*

Appendix……...…….……*IV*

Chapter I: Overview of the various storage elements..

1.1 Introduction : 1

1.2 What is Solar Energy and How is it Generated? 1

1.2.1 Solar Energy: …….. 1

1.2.2 How is Solar Energy Generated?..... 2

1.2.2.1 Photovoltaic (PV) Systems :…… 2

1.2.2.2 Solar Thermal Systems: 3

1.2.3 Advantages and Challenges of Solar Energy :[3]…… 3

1.3 Description of some types of storage elements and their characteristics: 4

1.3.1 Batteries (Regular Battery): 4

1.3.2 Solar Battery: 5

1.3.2.1 differences between regular batteries and solar batteries: 6

1.3.2.2 Kinds of batteries: 6

1.3.2.2.1 Lead battery: 6

1.3.2.2.2 Batterie AGM: 7

1.3.2.2.3 Lithium batteries:…… 8

1.3.2.2.4 Nickel-Cadmium (Ni-Cd) Batteries: 9

1.3.2.2.5 Nickel Hydrogen (Ni-H2) Batteries: 9

1.3.2.3 The Difference Between Types of Batteries:……. 10
1.3.3 Ultracapacitors (Supercapacitors):…… 11
1.3.3.1 Theoretical Advantages and Limitations of Ultracapacitors : 12
1.3.4 inertial wheels: 12
1.3.4.1 Advantages and Limitations of inertial wheels : 13
1.3.5 Hydrogen Storage: 14
1.4 Comparison of Energy Storage elements: 15
1.5 Conclusion : 16

Chapter II: Modeling of a solar battery.

2.1 Introduction: 17
2.2 The different equivalent schemes of a battery :…….. 18
2.2.1 Thevenin Model:…… 18
2.2.1.1 Variants of the Thevenin Model: 19
2.2.1.1.1 RC Network (Rp, Cp): 19
2.2.1.1.2 Dual RC Thevenin Model : 20
2.2.1.1.3 Hysteresis Thevenin Equivalent Circuit for Batteries:……. 21
2.2.1.2 Applications of the Thevenin Model:…… 23
2.2.1.3 Advantages and Limitations of the Thevenin Model: 23
2.2.2 Ideal Voltage Source Model : 23
2.2.3 Internal Resistance Model (Ohmic Model): 24
2.2.4 Dynamic Internal Resistance Model (DIRM): 25
2.2.5 General Nonlinear (GNL) Model : 26
2.2.6 Single Particle Model (SPM) : 28
2.2.7 Randles Circuit Model : 30
2.3 Comparison Between Equivalent Models: 32
2.4 Battery Performance Indicators: 33
2.4.1 State of charge (SOC): 33
2.4.2 State of health (SOH): 34
2.4.3 Depth of discharge definition (DOD): 36
2.4.4 End of Life (EOL):…… 37
2.4.5 State of Function (SOF): 37

2.5 Different techniques used to quantify the SOC: 37
2.5.1 Battery Voltage Method (Open Circuit Voltage - OCV): 37
2.5.1.1 OCV-SoC Curve: 38
2.5.2 The Recursive Least Squares (RLS) 39
2.5.2.1 Principle of Operation: 39
2.5.2.2 Advantages of the Recursive Least Squares (RLS) Algorithm: 40
2.5.3 Coulomb Counting Method:..... 40
2.5.3.1 Coulombic Efficiency and Its Impact: 41
2.5.3.2 Advantages of Coulomb Counting Method: 42
2.5.3.3 Challenges in the Coulomb Counting Method: 42
2.5.4 Kalman Filter Method: 43
2.5.4.1 State Model:..... 43
2.5.4.2 Measurement Model: 44
2.5.4.3 Kalman Filter Steps 44
2.5.5 Neural networks in battery state of charge estimation: 46
2.6 Conclusion:..... 48

Chapter III: Using three methods to estimate the state of charge. (Simulation).

3.1 Introduction: 49
3.2 Battery parameter identification : 50
3.3 State of Charge Estimation Methods: 52
3.3.1 Recursive Least Squares (RLS) Method: 52
3.3.1.1 Description of the scheme used in the simulation: 53
3.3.1.2 Simulation Results: 55
3.3.2 Coulomb based SOC algorithm: 60
3.3.3 proposition of an adaptive law to correct it: 62
3.3.3.1 Results of the Proposed SOC Estimation Method : 65
3.3.4 Kalman filter based SOC estimation:..... 69
3.3.4.1 Result of Simulation: 73
3.4 Conclusion: 76

List of Figures

List of Figures:

Chapter I

Figure 1-1 :Overview of Solar Energy: ……..1

Figure 1-2 :Photovoltaic effect at the cell level……..2

Figure 1-3 :Real solar panels……..2

Figure 1-4: Photovoltaic Systems Electrical model of a PV cell……2

Figure 1-5 :The operating principle of thermal solar panels……3

Figure 1-6 :Description of the interior of a battery……4

Figure 1-7 : Solar Battery……5

Figure 1-8 :How to Connect Solar Batteries……5

Figure 1-9: Types of lead-acid batteries ……7

Figure 1-10 : Schéma of batteries (NI-CD)……9

Figure 1-11 : Schéma of batteries (NI-H2……9

Figure 1-12 :Synoptic of an Ultracapacitor Module……11

Figure 1-13 :inertial wheels Model……13

Figure 1-14 : HYDROGEN ENERGY STORAGE SYSTEM……14

Chapter II

Figure 2-1 :Thevenin equivalent circuit 18

Figure 2-2 :Thevenin Battery Model with Polarization Effects 19

Figure 2-3 :Dual RC Thevenin Model 20

Figure 2-4 :The hysteresis phenomenon in a battery.[13] 21

Figure 2-5 :Thevenin electrical model with polarization effect 22

Figure 2-6 :Equivalent circuit of the battery (Static model) 23

Figure 2-7 :Discharge curve of a battery [7] 24

Figure 2-8 : Battery with Internal Resistance Model 25

Figure 2-9 :Battery block representation as a generic dynamic model [16] 26

Figure 2-10 :General Nonlinear (GNL) Model 27

Figure 2-11 :Sketch of the Single Particle Model concept [16] 29

Figure 2-12 :Equivalent Randles Circuit Model [17] 31

Figure 2-13 :Different ways a battery can degrade 34
Figure 2-14 : The capacity fade curve 35
Figure 2-15 :The open circuit voltage (OCV) and the state of charge (SOC) for a lithium-ion battery 38
Figure 2-16 :SoC estimations by CC method for low and severe measuring errors 41
Figure 2-17 :The noisy terminal voltage, current and process noises [21] 45
Figure 2-18:Estimations of the terminal voltage and the initial value of the SOC [21]..... 46

Chapter III

Figure 3-1 :Thevenin model with a polarization branch 50
Figure 3-2: Matlab/Simulink diagram for battery testing (RLS Method). 54
Figure 3-3 :The open-circuit voltage as a function of the state of charge. 57
Figure 3-4 :The state of charge as a function of the open-circuit voltage 58
Figure 3-5 :The Joule loss resistance as a function of the state of charge. 59
Figure 3-6 :The capacitance of the polarization branch as a function of the state of charge. .. 59
Figure 3-7 :Matlab/Simulink diagram for battery and Coulomb Counting (CC) method 60
Figure 3-8 :Results of the experiment 61
Figure 3-9 :Block diagram of the proposed method for SOC estimation 62
Figure 3-10 :Matlab/Simulink diagram for battery and Proposition of an adaptive law to correct the Coulomb Counting (CC) method 64
Figure 3-11 : Results of the first experiment 66
Figure 3-12 : Results of the second experiment 67
Figure 3-13 : Results of the third experiment 68
Figure 3-14 :Thevenin model with a polarization branch 69
Figure 3-15 :Principle block diagram of the Kalman filter [24] 71
Figure 3-16 :Computation steps of the EKF algorithm [24] 72
Figure 3-17 :OCV-SOC curve 73
Figure 3-18 :SOC estimation results 74
Figure 3-19 :Vb estimation results 74

List of Tables

List of Tables:

Table 1 :Advantages and Challenges of Solar Energy 3
Table 2:The fundamental differences between regular batteries and solar batteries 6
Table 3 :Technical Characteristics of the Lithium-Ion Battery 8
Table 4 :The Difference Between Types of Batteries 10
Table 5 :Advantages and Limitations of Ultracapacitors 12
Table 6:Advantages and Limitations of inertial wheels 13
Table 7 :Comparison of Energy Storage éléments 15
Table 8 :Comparison Between Equivalent Models 32
Table 9 :Importance of Estimating Battery State of Health (SOH). 36
Table 10 :Advantages of the Recursive Least Squares (RLS) Algorithm 40
Table 11 :Advantages and Disadvantages of Neural networks 47
Table 12 :Switching table 54
Table 13 : Identification résulte 56
Table 14 : Mean Absolute error of SOC Estimation 68
Table 15 : Comparison Between the Studied Methods 75

Symbols and notations

Symbols and notations:

IEA	International Energy Agency
CC	Coulomb Counting
OCV	Open Circuit Voltage
RLS	Recursive Least Square
BMS	Battery Management Systems
PI	Proportional-Integral
MAE	Mean Absolute Error
EKF	Extended Kalman Filters
UKF	Unscented Kalman Filters
ECM	Equivalent Circuit Models
SoC	State of Charge
SoH	State of Health
DoD	Depth of Discharge
SOF	State of Function
EOF	End of life
PV	Photovoltaic
DC	Direct current
AC	Alternating current
P	Positive electrode
N	Negative electrode
PbO_2	Lead dioxide
Pb	Lead
Lion-ion	Lithium-ion
H_2SO_4	Sulfuric acid
AGM	Absorbent Glass Mat
VRLA	Valve Regulated Lead Acid
UPS	Uninterruptible Power Supply systems
Ni-Cd	Nickel-Cadmium
Ni-H2	Nickel Hydrogen
ECMs	Equivalent circuit models

Eth	Thevenin voltage
Rth	Thevenin resistance
Rp	Polarization Resistor
Cp	Polarization capacitor
Vp	Polarization voltage
Ri	Internal resistance
V_{bat}	Battery voltage
V_{oc} , Ebat	Open circuit voltage .
Ib	Battery current (positive for discharge, negative for charge).
$VC_i(t)$	Voltage across the capacitor C_i in the i-th RC network.
V_P	Voltage across the RC network
R_2	Second RC network Resistor
C_2	Second RC network capacitor
V_{term}	Terminal voltage
SEI	Solid Electrolyte Interphase
V_H	Hysteresis term voltage
H	Cofficient of currant variation impact
EV	Electric Vehicle
ESS	Electrochemical storage systems
DIRM	Dynamic Internal Resistance Model
R0	Ohmic resistance
GNL	General Nonlinear
SPM	Single Particle
ϕ^T	Is called the regressor .
Θ	Is the parameter vector to be estimated .
y	The measured output .
$.\hat{y}$	The estimated output
$e(k)$	Error (the random noise).
λ	The forgetting factor .

P	Covariance matrix .
K	Filter gain .
IGBT	Insulated Gate Bipolar Transistor .
Ɣ	Adaptation gain .
δ	Correction parameter .
W(t)	System noise.
V(t)	Measurement noise .

General Introduction

General Introduction:

The early decades of the third millennium witnessed a steady increase in global energy consumption, with expectations for this upward trend to continue amid accelerating economic expansion and rising per capita electricity consumption across various regions. Reports from the International Energy Agency (IEA) indicate that fossil fuels (such as oil, coal, and gas) accounted for significant and varying proportions of the total energy consumed globally, and these natural resources are expected to be depleted within the next five decades.

Furthermore, the use of these resources is associated with the release of intensive carbon emissions, which aggravate global warming and environmental challenges, threaten ecological balance, and jeopardize energy security for future generations. In light of this, the **IEA** recommends accelerating the shift towards sustainable energy solutions as a strategic option.

In this context, the issue of supplying electricity to remote areas becomes evident, where traditional infrastructure faces difficulties in covering regions with challenging geographical features such as mountainous areas, isolated islands, desert plateaus, and remote regions with low population density. Therefore, it has become essential to develop innovative solutions based on renewable energy sources, such as solar cells, to ensure energy supply in these areas. It is well known that these energy sources are not continuous, and their availability is limited to specific periods, which requires storing the produced energy for use when the primary source is unavailable.

This brings us to the question: how can we store the generated energy, and what are the available storage systems?

With tremendous technological advancements in energy storage systems, particularly those integrated with solar cells, batteries have assumed a central role in critical applications such as zero-emission vehicles, photovoltaic systems, smart drones, and portable electronic devices.

Monitoring battery performance indicators in such systems is of utmost importance to ensure their effectiveness. So, what are these indicators, and what are their technical characteristics?

These indicators not only contribute to improving energy management but also help maintain the operational stability of the system by preventing it from operating beyond safe limits. One of the most critical indicators is the **State of Charge (SOC)**, which plays an essential role in

control systems, energy management, and protecting the system's components from unsafe operating conditions.

Since **SOC** cannot be directly measured using traditional sensors, this raises several questions about this indicator, its function, and how it can be calculated?

This challenge has led to extensive research efforts to develop accurate and reliable estimation methods. These methods vary in their mathematical structures, computational requirements, and accuracy under different operating conditions.

Traditional techniques include methods based on voltage and current measurements, such as **Coulomb Counting (CC)** and **Open Circuit Voltage (OCV)**. These are relatively simple but are prone to cumulative errors and are affected by thermal and chemical factors.

For example A study by Agus Kustiman, and others [1], the study aims to enhance the accuracy of **SOC** estimation in Battery Management Systems (BMS), particularly for electric vehicles, by proposing a hybrid method combining Coulomb Counting (CC), Recursive Least Square (RLS) for identifying dynamic battery model parameters (Thevenin model), and a Proportional-Integral (PI) controller to correct errors from inaccurate initial SOC values , the experimental results showed that the proposed method significantly outperformed the conventional CC method, effectively correcting estimation errors and converging to the actual SOC within 200 seconds. It achieved a Mean Absolute Error (MAE) of just 0.498%, while the CC-only method resulted in estimation errors ranging from 2% to 35%. The study concluded by recommending further optimization of PI controller parameters through systematic tuning methods to improve SOC estimation accuracy and reliability.

To address such challenges, more advanced and complex estimation techniques have emerged in recent years, including various types of **Kalman Filters** (such as EKF and UKF), **Equivalent Circuit Models (ECM)**, and dynamic models based on differential equations.

The accuracy of these estimation techniques plays a critical role in smart control systems, which require immediate and effective responses to any changes in environmental conditions or load demands.

This thesis aims to improve SOC estimation techniques by using advanced methods and technologies that ensure high performance and accurate prediction of the state of charge in these systems.

This thesis consists of three main chapters in addition to the conclusion:

- **Chapter One:** Provides an overview of various storage elements and emphasizes the importance of batteries as the primary source of energy storage. It reviews the different types of batteries used in various applications and explains how storage systems manage energy flows.
- **Chapter Two:** Focuses on modeling solar batteries, demonstrating how to accurately model solar batteries using mathematical equations and evaluate their performance based on factors such as temperature, lifecycle, and discharge rate , this chapter provides a detailed exploration of battery modeling of the different equivalent schemes of a battery, such as the Thevenin equivalent circuit with their variants, and other advanced models that offer valuable tools for capturing the dynamic behavior of batteries under various operating conditions. Additionally, the definitions of critical battery metrics State of Charge (SoC), State of Health (SoH), and Depth of Discharge (DoD).
- **Chapter Three:** Discusses practical methods for estimating the State of Charge (SOC), analyzing the main techniques used for SOC estimation, such as Coulomb Counting, Kalman Filters, and Equivalent Circuit Models, along with a discussion on the effectiveness of these methods in real-world applications.

Throughout these chapters, a detailed analysis is presented of the various methods used to estimate the SOC of solar batteries, along with a review of the advantages and disadvantages of each method in practical contexts.

The focus is placed on how these methods can be enhanced to meet future needs and provide sustainable and reliable solutions for standalone systems that rely on solar power.

Finally, the study concludes with a comprehensive summary of the main research findings, offering practical recommendations for future studies in this field and identifying emerging trends in SOC estimation techniques.

Chapter I: Overview of the various storage elements

1 Chapter I: Overview of the various storage elements.

1.1 Introduction :

Batteries are currently considered among the most prominent and widely used energy storage sources across a broad range of modern applications, including electric and hybrid vehicles, renewable energy systems, and marine energy systems. They play a vital role as a backup power source in photovoltaic and wind energy conversion systems, where they are used to store excess energy generated during peak periods and supply it again during times of low production or outages, such as stationary periods or nighttime.

This chapter aims to address the first question raised in the general introduction by analyzing and discussing limited-power energy sources currently in use, namely batteries and supercapacitors. It also explores the various battery technologies, classifies their types, and reviews their technical characteristics, in addition to presenting the most well-known practical models that serve as effective solutions for energy storage requirements in modern systems.

1.2 What is Solar Energy and How is it Generated?

1.2.1 Solar Energy:

The amount of sunlight that strikes the earth's surface in an hour and a half is enough to handle the entire world's energy consumption for a full year. Solar technologies convert sunlight into electrical energy either through photovoltaic (PV) panels or through mirrors that concentrate solar radiation, this energy can be used to generate electricity or be stored in batteries or thermal storage.[4]

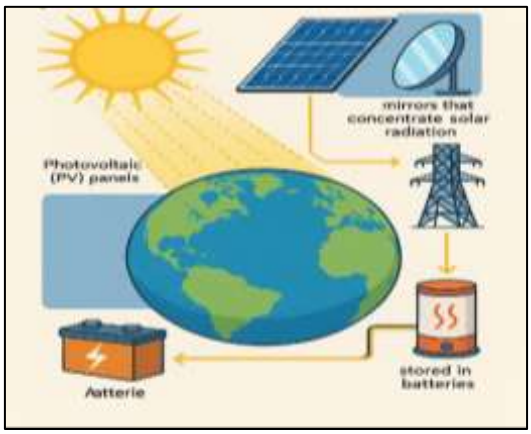

Figure 1-1 :Overview of Solar Energy: Its Generation and Storage Components

1.2.2 How is Solar Energy Generated?

There are two main technologies used to generate solar energy:

1.2.2.1 Photovoltaic (PV) Systems :

These systems convert sunlight directly into electricity using solar panels made of semiconductors like silicon, Its working principle is as follows:

When sunlight hits the solar cells, typically made of silicon, the energy from the light excites the electrons, generating a direct current (DC). This current is then passed through an inverter, which converts it into alternating current (AC), the form of electricity commonly used in homes and businesses. The electricity produced can either be used immediately or stored in batteries for later use. This technology is commonly utilized in rooftop solar panels, largescale solar farms, and portable solar-powered devices.

The electrons and holes are separated by the P(positive electrode)-N(negative electrode) junctions within the cell, generating a voltage difference (photovoltaic voltage) See Figure 1-2.

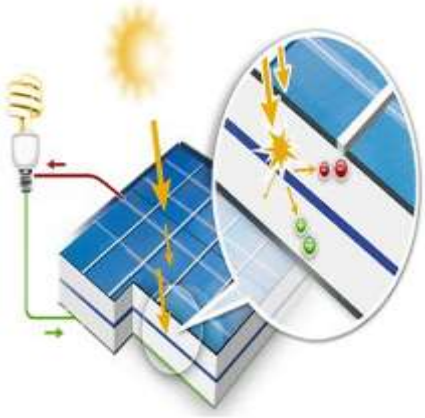

Figure 1-2 :Photovoltaic effect at the cell level[19]

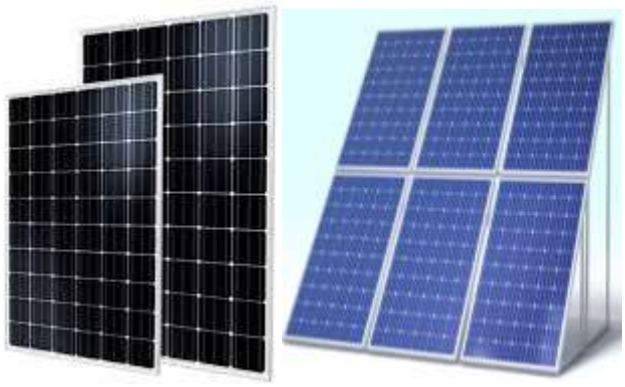

Figure 1-3 :Real solar panels

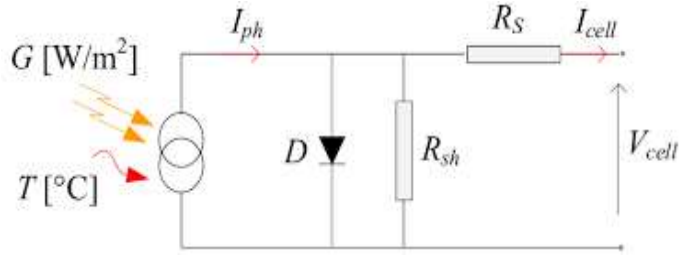

Figure 1-4: Photovoltaic Systems Electrical model of a PV cell.[19]

1.2.2.2 Solar Thermal Systems:

A thermal solar collector is designed to convert the heat energy radiated by the sun into thermal energy. It consists of a glazed box containing a metal plate and black metallic tubes (absorbers). The energy collected by the absorbers is transferred to a heat transfer fluid circulating through pipes, which serve to transport the heat from the collector to the point of use. To better understand the operating principle of these panels, see the following image (figure 1-5). [6]

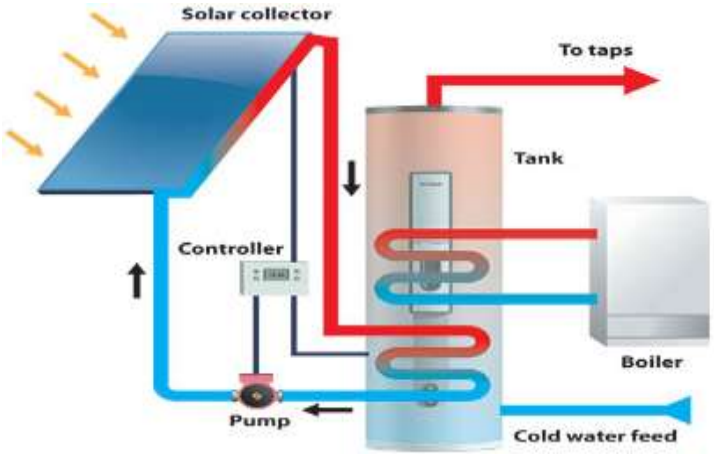

Figure 1-5 :The operating principle of thermal solar panels [5]

1.2.3 Advantages and Challenges of Solar Energy :[6]

Category	Item
Advantages of Solar Energy	Renewable & Sustainable
	Cost Savings
	Low Maintenance
	Eco-Friendly
	Energy Independence
Challenges	High Upfront Cost
	Weather Dependent
	Costly Storage

Table 1 :Advantages and Challenges of Solar Energy

1.3 Description of some types of storage elements and their characteristics:

1.3.1 Batteries (Regular Battery):

A **battery** is a device that converts the chemical energy contained in its active materials directly into electric energy by means of an electrochemical oxidation-reduction (redox) reaction. In the case of a rechargeable system, the **battery** is recharged by a reversal of the process. This type of reaction involves the transfer of electrons from one material to another through an electric circuit. In a nonelectrochemical redox reaction, such as rusting or burning, the transfer of electrons occurs directly and only heat is involved. As the **battery** electro chemically converts chemical energy into electric energy, it is not subject, as are combustion or heat engines, to the limitations of the Carnot cycle dictated by the second law of their modynamics. **Batteries**, therefore, are capable of having higher energy conversion efficiencies. [4]

While the term ‘‘**battery**’’ is often used, the basic electrochemical unit being referred to is the ‘‘cell.’’ A **battery** consists of one or more of these cells, connected in series or parallel, or both, depending on the desired output voltage and capacity.[5]

The cell consists of three major components:

1. The anode or negative electrode (-) the reducing or fuel electrode: which gives up electrons to the external circuit and is oxidized during the electrochemical reaction. 2. The cathode or positive electrode (+) the oxidizing electrode: which accepts electrons from the external circuit and is reduced during the electrochemical reaction.[4],As shown in the following (Figure 1-6).

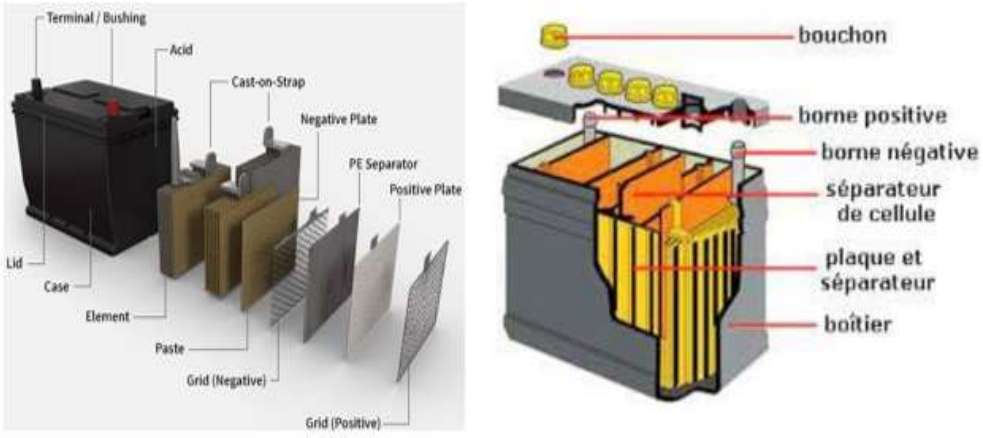

Figure 1-6 :Description of the interior of a battery[4][11]

1.3.2 Solar Battery:

Batteries Except in a grid-tie system, where the solar array connects directly to an inverter, solar panels rarely power electrical equipment directly. This is because the amount of power the solar panel collects varies depending on the strength of sunlight. This makes the power source too variable for most electrical equipment to cope with. In a grid-tie system, the inverter handles this variability: if demand outstrips supply, you will get power from both the grid and your solar system. For a stand-alone or a grid fallback system, batteries store the energy and provide a constant power source for your electrical equipment. Typically, this energy is stored in 'deep cycle' lead acid batteries. These look similar to car batteries but have a different internal design. This design allows them to be heavily discharged and recharged several hundred times over. Most lead acid batteries are 6-volt or 12-volt batteries and, like solar panels, these can be connected together to form a larger battery bank. Like solar panels, multiple batteries used in series increase the capacity and the voltage of a battery bank. Multiple batteries connected in parallel increase the capacity whilst keeping the voltage the same , The batteries are connected as shown in (Figure1-8).[6]

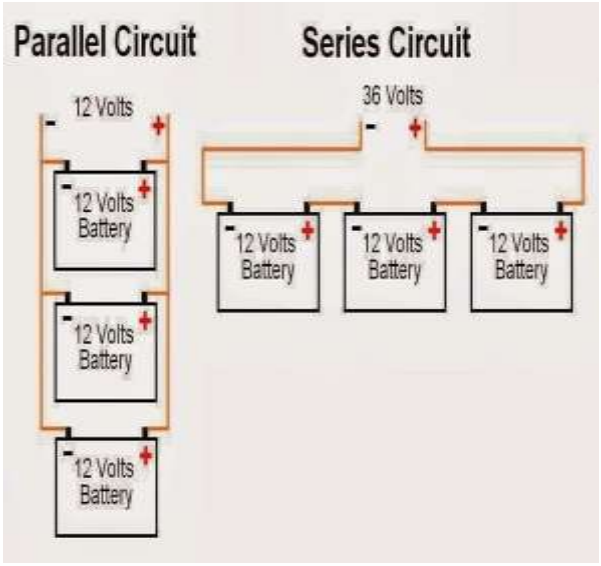

Figure 1-8 :How to Connect Solar Batteries

Figure 1-7 : Solar Battery

1.3.2.1 differences between regular batteries and solar batteries:

The following table highlights the fundamental differences between regular batteries and solar batteries:

Feature	Regular Battery	Solar Battery
Purpose	General use	Designed for solar systems
Charge cycles	Fewer	More
Deep discharge	Not suitable	Designed to handle it
Heat resistance	Lower	Higher
Lifespan	Shorter	Longer

Table 2:The fundamental differences between regular batteries and solar batteries

1.3.2.2 Kinds of batteries:

1.3.2.2.1 Lead acid battery:

It is composed of two electrodes (positive and negative) and an electrolyte. The positive electrode is made of lead dioxide (PbO_2), and the negative electrode is made of lead (Pb).[6]

The electrolyte is a sulfuric acid solution (H_2SO_4), which enables the flow of ions between the two electrodes and generates a current. The density of the electrolyte decreases during discharge as the battery supplies current, and the active materials are converted into sulfate and water.

Lead-acid accumulators are divided into two main categories: open batteries (Vented Batteries) and sealed batteries (Valve Regulated Lead Batteries).

There are several types of this battery, as illustrated in (Figure 1-9).

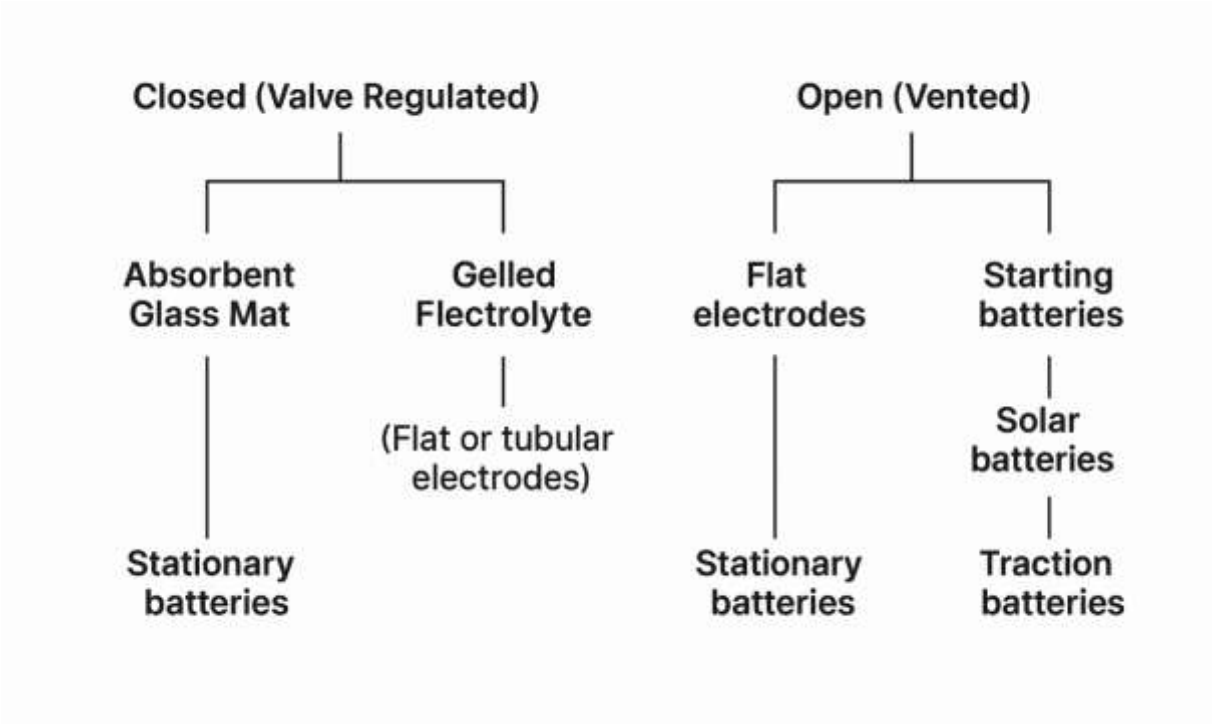

Figure 1-9: Types of lead-acid batteries [11]

1.3.2.2.2 Battery AGM:

An AGM battery (Absorbent Glass Mat) is a type of Valve Regulated Lead Acid (VRLA) battery. It uses a glass mat separator to hold the electrolyte, which is absorbed into the mat rather than being in liquid form. This design offers several advantages, including:

- **Maintenance-Free**: Sealed design eliminates the need to add water.
- **Spill-Proof**: The absorbed electrolyte reduces the risk of leaks, allowing for versatile installation.
- **Low Self-Discharge**: Retains charge for longer periods when not in use.
- **Vibration Resistance**: The compact and sealed construction improves durability in harsh conditions.
- **High Performance**: Provides consistent power delivery and can handle high discharge and recharge cycles.

AGM batteries are commonly used in solar systems, UPS systems, automotive applications, and motorcycles due to their reliability and efficiency.

1.3.2.2.3 Lithium batteries:

The increasing use and growing diversity of electrical applications have led to the development of new storage technologies. Research and development efforts have resulted in the emergence of new electrochemical storage technologies, such as Redox systems, hydrogen storage systems, and lithium batteries. There are three main families of lithium batteries: Metallic Lithium, Lithium-Ion, and Lithium-Polymer.

Characteristic	Typical Value
Lifespan	5 to 10 years
Cycle life	500 to 2000 cycles
Charge/discharge efficiency	90 to 95%
Self-discharge rate (% per month)	1 to 5%
Nominal voltage per cell	3.6 to 3.7 V
Internal resistance	20 to 100 $m\Omega$
Operating temperature (°C)	0 to 45 °C (up to 60 °C for some models)
Gravimetric energy density	150 to 250 Wh/kg
Volumetric energy density	250 to 700 Wh/l
Charging time	1 to 4 hours
Maintenance	Low to none (no regular maintenance required)

Table 3 :Technical Characteristics of the Lithium-Ion Battery

1.3.2.2.4 Nickel-Cadmium (Ni-Cd) Batteries:

They offer superior performance to lead in terms of capacity and lifespan. However, they require a very clean charging power source and their price is significantly higher than lead batteries (about 1.5 times).

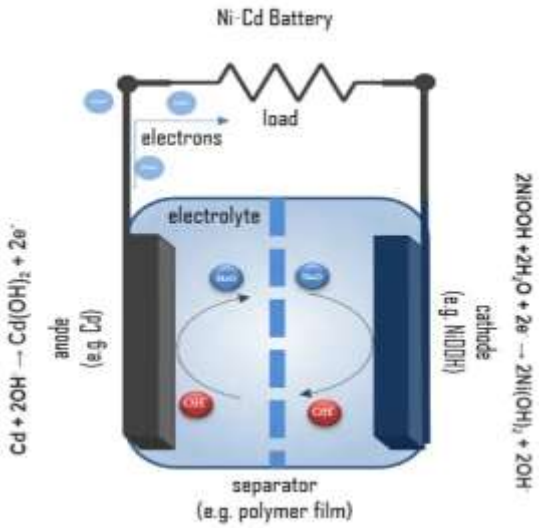

Figure 1-10 : Schéma of batteries (NI-CD)

1.3.2.2.5 Nickel Hydrogen (Ni-H2) Batteries:

Since 1964, H2/O2 fuel cells have been commonly used in space applications (satellites and shuttles). On satellites, they serve as accumulators to store the excess electricity provided by solar panels, which is then released during eclipses (a large number of cycles)

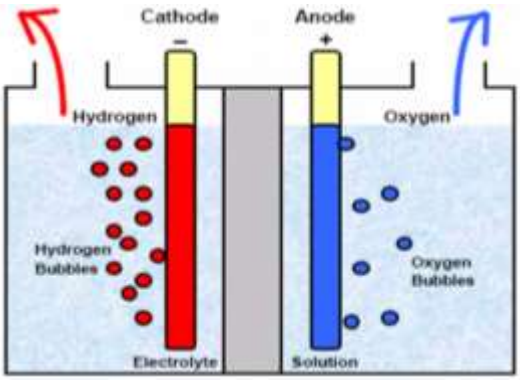

Figure 1-11 : Schéma of batteries (NI-H2)

1.3.2.3 The Difference Between Types of Batteries:

The following table highlights the fundamental differences between conventional batteries and solar batteries:

Property	Lead Acid	AGM (Absorbent Glass Mat)	Lithium	Ni-Cd (Nickel-Cadmium)	Ni-H2 (Nickel-Hydrogen)
Energy Density (Wh/kg)	30-50	40-60	150-250	45-80	70-100
High Power Capability	Good (moderate current flow)	Good (higher current flow than lead acid)	Excellent (very high power output)	Good (high power output)	Very good
Cycle Life	300-500	500-1000	1000-5000	1000-2000	2000-3000
Service Life	3-5 years	5-7 years	8-15 years	10-15 years	10-15 years
Nominal Cell Voltage (V)	2.0	2.0	3.2-3.7	1.2	1.2
Operating Temperature Range (°C)	-20 to 50	-20 to 50	-20 to 60	-40 to 70	-40 to 70
Estimated Cost (€/kW)	150-300	200-400	400-800	300-600	500-900
Common Applications	Vehicles, backup power, UPS	Vehicles, UPS, emergency systems	Phones, electric vehicles, renewable energy	Aviation, industrial applications, solar power	Satellites, space, specialized applications
Maintenance	Requires regular inspection and refilling	Low (sealed, maintenance-free)	Very low (mostly maintenance-free)	Moderate (requires periodic conditioning)	Low
Advantages	Low cost, mature technology	Less leakage, better performance than traditional lead acid	High energy density, long life, lightweight	High temperature tolerance, long life	Long life, stable performance in harsh conditions
Disadvantages	Heavy, short life, ongoing maintenance	Higher cost than traditional lead acid	High cost, sensitive to heat	Cadmium toxicity, memory effect	High cost, larger size and weight

Table 4 :The Difference Between Types of Batteries

1.3.3 Ultracapacitors (Supercapacitors):

In general, capacitor is a device to store the charge in an electric circuit. Basically, a capacitor is made up of two conductors separated by an insulator called dielectric. The dielectric can be made of paper, plastic, mica, ceramic, glass, a vacuum or nearly any other nonconductive material. Some capacitors are called Electrolytic in which the dielectric is aluminum foilconductor coated with oxide layer.

Ultracapacitors can be defined as an energy storage device that stores energy electrostatically by polarizing an electrolytic solution. Unlike batteries no chemical reaction takes place when energy is being stored or discharged and so ultracapacitors can go through hundreds of thousands of charging cycles with no degradation.

Ultracapacitors are also known as double-layer capacitors or supercapacitors.[7]

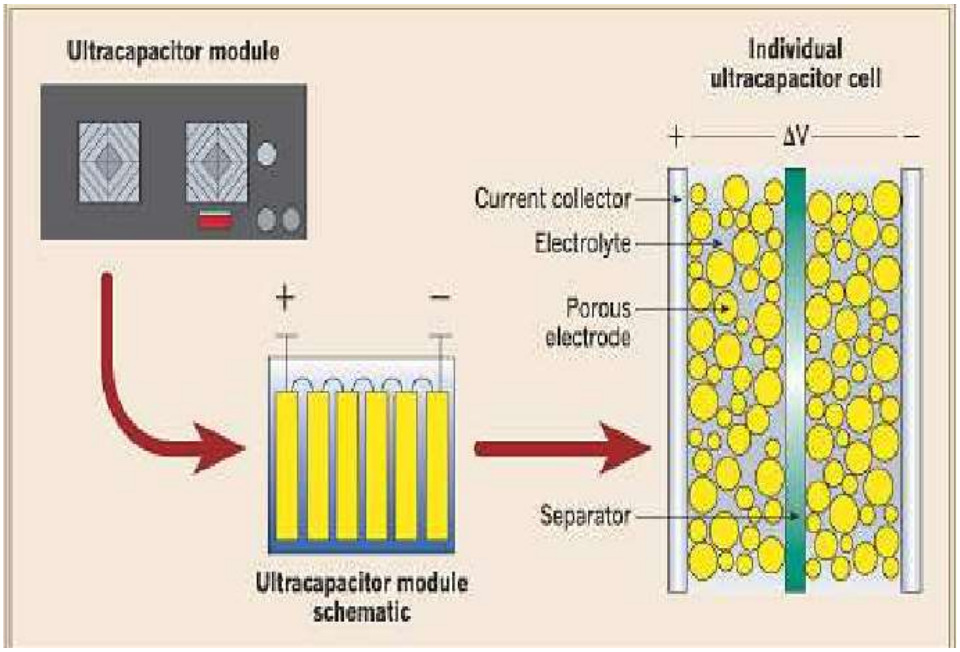

Figure 1-12 :Synoptic of an Ultracapacitor Module[7]

The use of supercapacitors in the automotive sector specifically addresses the following needs:[7]

- Starting and coping with low-temperature constraints.
- Assistance during acceleration and energy recovery.
- Powering auxiliary systems.

1.3.3.1 Theoretical Advantages and Limitations of Ultracapacitors :

Theoretical Advantages	Theoretical Limitations
Very Fast Charging and Discharging: Can charge/discharge in seconds or less.	Low Energy Density: Stores much less energy per unit weight/volume.
Extremely Long Lifespan: Tolerates hundreds of thousands of cycles.	Low Voltage per Cell: Requires many cells in series to reach higher voltages.
High Energy Efficiency (90–95%): Minimal energy loss during operation.	High Self-Discharge Rate: Loses charge over time even when idle.
Environmentally Friendly: No toxic materials.	Relatively High Cost: Expensive for large-scale energy storage.
Good Thermal Performance: Works efficiently across various temperatures.	

Table 5 :Advantages and Limitations of Ultracapacitors

1.3.4 inertial wheels:

In the field of electricity, inertial wheels, also referred to as flywheels, are devices used for energy storage, stabilization, and power management. They operate by storing kinetic energy in the rotational motion of a mass and converting this energy back into electricity when required. This makes them a crucial component in modern electrical systems, especially in applications requiring rapid energy delivery, power quality improvement, or grid stabilization.[8]

The main components of an electromechanical inertial energy storage device are typically represented schematically (see Figure 1-13).

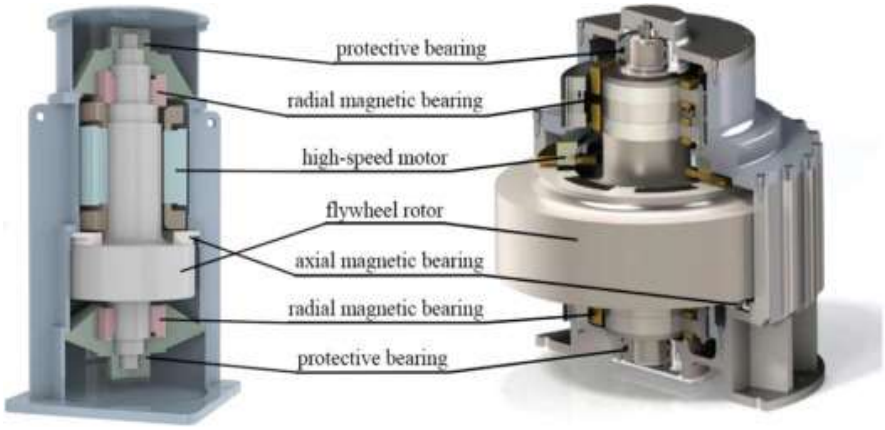

Figure 1-13:inertial wheels Model[8]

1.3.4.1 Advantages and Limitations of inertial wheels :

Advantages	Limitations
Fast Response Time	Low Energy Density.
High Efficiency (85–95%)	Mechanical Losses.
Durability and Longevity.	High Initial Cost.
Eco-Friendly.	Risk of Failure.
Scalability.	

Table 6:Advantages and Limitations of inertial wheels

1.3.5 Hydrogen Storage:

Hydrogen storage is a major challenge in the development of the hydrogen economy due to its physical and chemical properties. The main methods for hydrogen storage are as follows:

1. **Compressed Hydrogen Storage:**
   Hydrogen is stored in high-pressure tanks, typically between 350 and 700 bar. This method is commonly used in applications such as fuel cell vehicles.

2. **Liquefied Hydrogen Storage:**
   Hydrogen is cooled to extremely low temperatures (-253°C) to become a liquid, increasing its volumetric energy density. This method is used in applications that require high energy density.

3. **Solid-State Storage:**
   Hydrogen is absorbed in solid materials such as metal hydrides or porous carbon materials. This method provides high safety and good energy density, but requires the development of advanced materials that allow hydrogen absorption and release under suitable pressure and temperature conditions.

Each method is used depending on the application, whether in transportation, renewable energy storage, or industrial use. Ongoing scientific research continues to improve the efficiency, safety, and cost of these methods, enhancing hydrogen's role in the future of energy.[9]

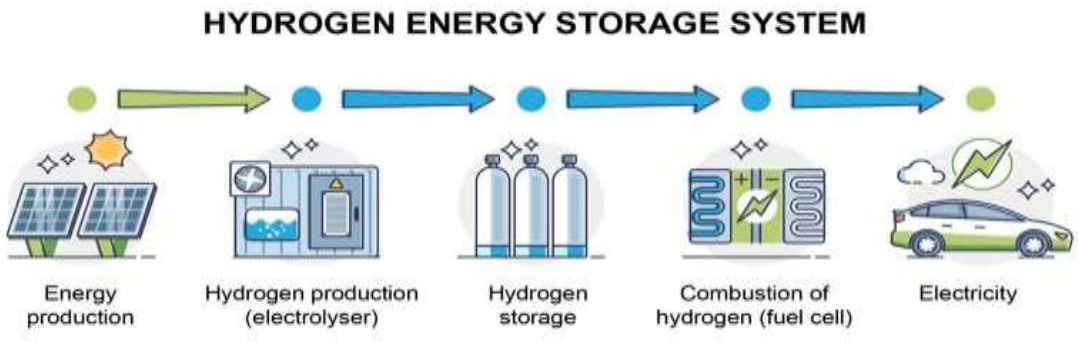

Figure 1-14 : HYDROGEN ENERGY STORAGE SYSTEM [9]

1.4 Comparison of Energy Storage elements:

Type	Capacitor	Battery	Flywheel	Compressed Air	Thermal Storage	Hydrogen Storage
Energy Density (Wh/kg)	Low (~0.1)	Medium (~100–250)	Medium (~20–80)	Medium (~30–60)	Medium to High (~50–150)	High (~120–500)
Power Density (W/kg)	Very high (>10,000)	Medium (~200–2,000)	High (~500–10,000)	Low (~100–500)	Low to Medium	Low to Medium
Efficiency	High (~95–99%)	Medium (~70–95%)	High (~85–95%)	Low (~40–70%)	Medium (~50–90%)	Low (~30–50%)
Response Time	Instantaneous	Seconds to minutes	Milliseconds to seconds	Seconds to minutes	Minutes to hours	Minutes to hours
Cycle Life	Very high (>1M)	Medium (~1k–10k)	High (~100k)	High	High	Medium
Approx. Cost (€/kWh)	~10,000–20,000 €	~100–300 €	~500–2,000 €	~20–60 €	~10–50 €	~300–1,000 €
Main Advantages	Fast charge/discharge	Good energy density	Reliable and durable	Low-cost for large scale	Good for load shifting	Clean fuel for long-term
Main Disadvantages	Low energy capacity	Degradation over time	Requires maintenance	Low efficiency	Temperature-dependent	Difficult to store/transport

Table 7 :Comparison of Energy Storage éléments

1.5 Conclusion :

This chapter provides a detailed description of various energy storage technologies and their characteristics, including batteries, supercapacitors, flywheels, and hydrogen storage.

These elements collectively form the foundation for understanding energy storage systems and their vital role in modern electrical and renewable energy applications.

It begins with a comprehensive analysis of the first source studied in this thesis, namely batteries, elucidating their operational principles and different types.

Finally, we highlighted the differences between the various energy storage elements.

Chapter II: Modeling of a solar battery

2 Chapter II: Modeling of a solar battery.

2.1 Introduction:

In renewable energy systems, particularly in photovoltaic applications, the integration of batteries is essential to ensure energy availability during periods of low or no solar irradiance. Accurate modeling of battery behavior is crucial for designing reliable and efficient energy storage systems. This chapter presents a comprehensive overview of the modeling approaches used to represent solar battery dynamics and performance.

The behavior of batteries is inherently nonlinear and time-dependent, influenced by factors such as temperature, aging, charge/discharge rates, and internal chemical reactions. To capture these dynamics, various equivalent electrical circuits have been developed, ranging from simple resistance-capacitance networks to more complex representations like the Thevenin and hysteresis-based models.

In addition to circuit-based modeling, this chapter explores essential battery parameters such as the **State of Charge (SOC)**, **State of Health (SOH)**, **Depth of Discharge (DOD)** , **End of life (EOL) and State of Function (SOF)** , which are key indicators of battery performance and lifespan. Several techniques used to estimate SOC ranging from Coulomb counting to advanced estimation algorithms , are also discussed.

By understanding and comparing these models, the reader will gain insight into how batteries behave under different conditions .

2.2 The different equivalent schemes of a battery :

There are different types of equivalent schemes for modeling a battery, each of which has its strengths and weaknesses. The equivalent Thevenin scheme is the most common, but others, such as Randles Model or Electrochemical, can be used depending on the needs.

Equivalent circuit models (ECMs) are widely used to represent a battery's electrical behavior. These models approximate the battery's voltage, current, and dynamic response using circuit elements like resistors, capacitors, and voltage sources. Below are some common equivalent battery schemes :

2.2.1 Thevenin Model:

The Thevenin equivalent circuit is a simple model used to represent a battery or any other electrical source with a voltage source in series with a resistance. A battery can be represented using the Thevenin voltage (Eth) and Thevenin resistance (Rth) as shown in (Figure 2-1). This model is particularly useful when we need to simplify complex circuits and analyze their response with a connected load.

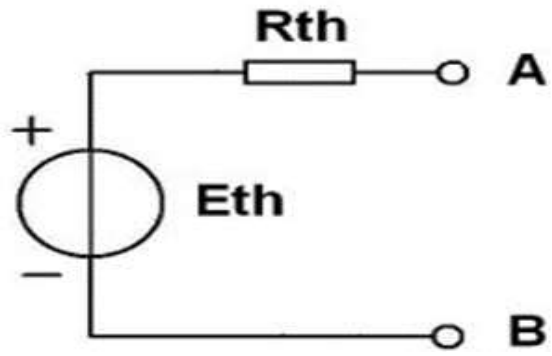

Figure 2-1 :Thevenin equivalent circuit[21]

In the Thevenin equivalent circuit:

- Eth : is the equivalent voltage of the battery.
- Rth : is the equivalent resistance representing the internal resistance of the battery (Joule Losses).

2.2.1.1 Variants of the Thevenin Model:

The Thevenin model has three types, which will be explained as follows :

2.2.1.1.1 RC Network (Rp, Cp):

- The R_1 C_1 network models transient voltage behavior caused by electrochemical processes inside the battery.
- R_1 represents polarization resistance, accounting for voltage delays due to charge redistribution.
- C_1 model's capacitance effects related to charge diffusion in active materials.
- This RC network explains slow voltage recovery after a current change.

Polarization Effects **,** as shown in (Figure 2-2) :

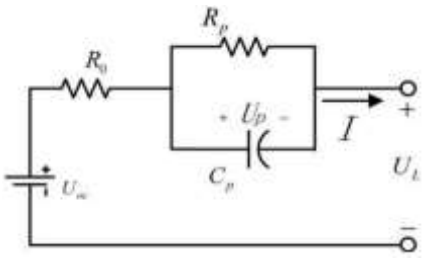

Figure 2-2 :Thevenin Battery Model with Polarization Effects [21]

The **RC** network (**Rp, Cp**) is a fundamental component used in battery models, especially in Thevenin-based models, to represent the transient behavior of the battery during charging or discharging. This network consists of a resistor **Rp** and a capacitor **Cp**. During discharge, the internal resistance **R0** may increase due to changes in electrode and electrolyte reactions, which leads to a reduction in the available current **Ib.** During charging, this resistance gradually decreases as the battery returns to its original state.

The resistor **Rp** represents the internal energy loss caused by current flow, while the capacitor **Cp** reflects the battery's ability to store and release charge. The voltage **Vp** represents the instantaneous voltage resulting from the interaction between **Rp** and **Cp**. This network helps accurately model the gradual change in voltage and simulates the voltage relaxation phenomenon that occurs when the load suddenly changes.

The **RC** network is widely used to represent voltage response over time, and multiple (**Rp, Cp**) pairs can be used to increase modeling accuracy. This makes the model suitable for Battery Management System (**BMS**) applications, which require a balance between simplicity and

accuracy. Moreover, this model enables precise analysis of battery indicators such as State of Charge (**SOC**) and State of Health (**SOH**) in a simplified manner.

The battery terminal voltage V_{bat} is given by:

$$V_{bat} = V_{oc} - Ib.R_0 - V_P \quad \text{(II.1)}$$

where:

V_{oc} : is the open circuit voltage .

Ib : is the battery current (positive for discharge, negative for charge).

V_P : is the voltage across the RC network, governed by:

$$\frac{dV_P}{dt} = -\frac{V_P}{R_P C_P} + \frac{Ib}{C_P} \quad \text{(II.2)}$$

2.2.1.1.2 Dual RC Thevenin Model :

Extends the Thevenin model by adding a second RC network (R_2, C_2).

Captures both fast and slow dynamic behaviors, improving accuracy.

Suitable for lithium-ion batteries with complex transient responses.

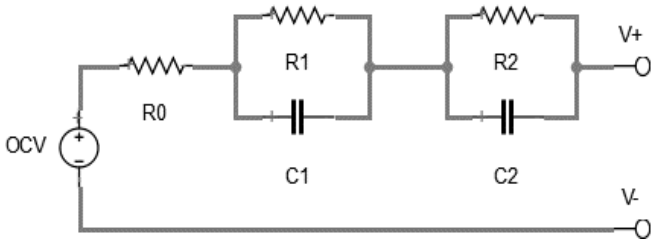

Figure 2-3 :Dual RC Thevenin Model[21]

- ✓ **Two RC Networks**:
  - **(R_1, C_1)**: Captures fast transient behavior (e.g., surface charge effects).
  - **(R_2, C_2)**: Captures slower dynamic behavior (e.g., diffusion processes inside electrodes).

✓ **Mathematical Model:** The voltage across each RC branch is governed by:

$$\frac{dV_{RC1}}{dt} = -\frac{1}{R_1 C_1} V_{RC1} + \frac{1}{C_1} I(t) \quad \text{(II.3)}$$

$$\frac{dV_{RC2}}{dt} = -\frac{1}{R_2 C_2} V_{RC2} + \frac{1}{C_2} I(t) \quad \text{(II.4)}$$

Then the terminal voltage is:

$$V_{term} = OCV - Ib.R_0 - (V_{RC1} + V_{RC2}) \quad \text{(II.5)}$$

2.2.1.1.3 Hysteresis Thevenin Equivalent Circuit for Batteries:

Hysteresis in lithium-ion batteries within the Thevenin model refers to the difference between the charge and discharge curves at the same state of charge (SOC), caused by nonlinear effects and changes in electrochemical reactions. This phenomenon leads to energy loss and reduces the accuracy of battery state estimation (figure 2-4). [14]

Hysteresis is undesirable as it results in energy loss during each charge / discharge cycle. Unfortunately, many new battery concepts that promise significant increases in energy density including those based on displacement and conversion reactions or anion-redox mechanisms suffer from severe hysteresis, which hinders their commercialization and practical use.[14]

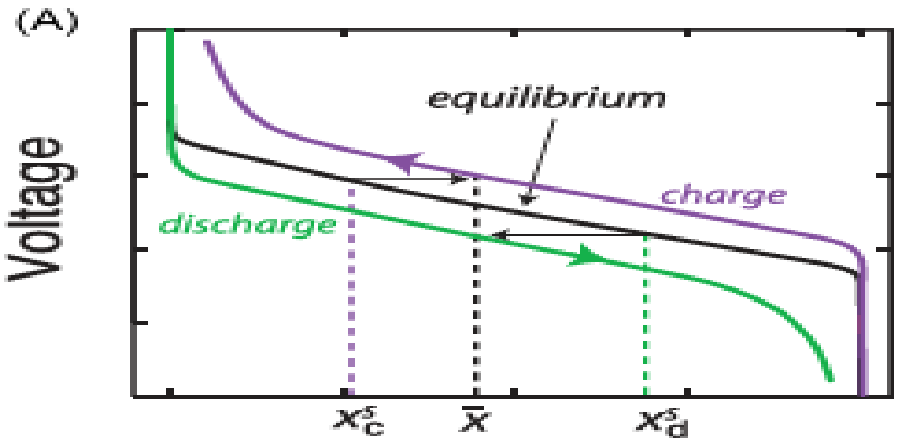

Figure 2-4 :The hysteresis phenomenon in a battery.[10][14]

During charging: The voltage is higher than expected.

During discharging: The voltage is lower than expected.

- As shown in the figure2-5:

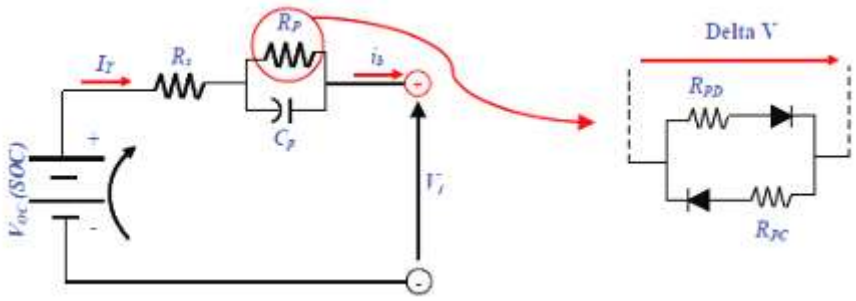

Figure 2-5 :Thevenin electrical model with polarization effect[11]

✓ **Causes of Hysteresis:**

Hysteresis is caused by several factors, including:

- Ion redistribution within the electrolyte.
- Slow electrochemical reactions (e.g., formation of the Solid Electrolyte Interphase - SEI).
- Capacitive effects and energy storage in the electrode structure.

✓ **Hysteresis Thevenin Model:**

To include hysteresis in the Thevenin model, different approaches can be used:

- **Adding a Hysteresis Voltage**

The battery voltage equation is modified by introducing a hysteresis term V_H :

$$V_{bat} = V_{OC} - I.R_{0-}V_{RC+}V_H \quad (II.6)$$

V_H : a Hysteresis Voltage

A simple approach expresses V_H as: $V_H = H.\mathrm{sgn}(I)$ (II.7)

- **Thevenin Model with an Additional RC Circuit**

A second RC network is added to capture hysteresis dynamics:

$$V_H = R_H I + V_{H,RC} \quad (II.8)$$

This model is more accurate than the simple hysteresis voltage approach but requires additional computation.

2.2.1.2 Applications of the Thevenin Model:

The Thevenin model is widely used in:

- Electric Network Analysis : used to simplify complex networks into a single voltage source and internal resistance, making it easier to calculate current or voltage in specific parts of the circuit.
- Battery Management Systems (BMS): Real-time monitoring of SOC , SOH and DOD.
- Electric Vehicle (EV) battery modeling: Predicting battery voltage under load.
- Renewable energy storage systems (solar, microgrids, off-grid applications).
- Battery simulation tools (MATLAB/Simulink, PSpice, etc.).

2.2.1.3 Advantages and Limitations of the Thevenin Model:

✓ **Advantages:**

+ Simple and computationally efficient, ideal for real-time applications.
+ Captures transient voltage response (voltage drop and recovery).
+ Works for various battery chemistries (Lithium-ion, Lead-acid, etc.).
+ Used in SOC and SOH estimation for battery management systems (BMS).

✓ **Limitations:**

− Does not capture long-term aging effects or degradation over cycles.
− Parameters vary with SOC and temperature, requiring frequent recalibration.
− Cannot model complex diffusion processes, limiting accuracy for high-capacity batteries.

2.2.2 Ideal Voltage Source Model :

The battery is modeled as an ideal voltage source in series with the internal resistance of the battery, as shown in the figure2-6:

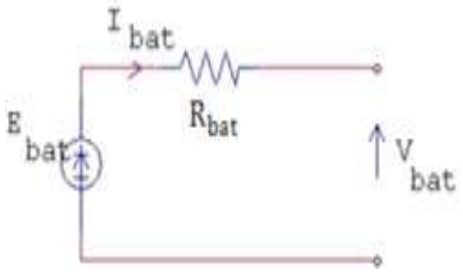

Figure 2-6 :Equivalent circuit of the battery (Static model) [11]

To calculate the battery voltage, the following equation is used:

$$V_{bat} = E_{bat} - R_{bat} \times I_{bat} \quad \text{(II.9)}$$

Ebat is the open-circuit voltage, **Rbat** is the internal resistance, and **Ibat** is the current supplied by the battery , A positive current indicates discharge, while a negative current indicates charging, This model is generally referred to as the **CIEMAT model**, based on the electrical diagram of the battery's electrochemical model , The battery is then represented by two components: a voltage source and an internal resistance **Ri**, whose characteristics depend on several parameters such as **temperature** and **state of charge**.[5]

In this model, three zones (of **SOC**) are distinguished , As shown in the following figure(2-7):[6]

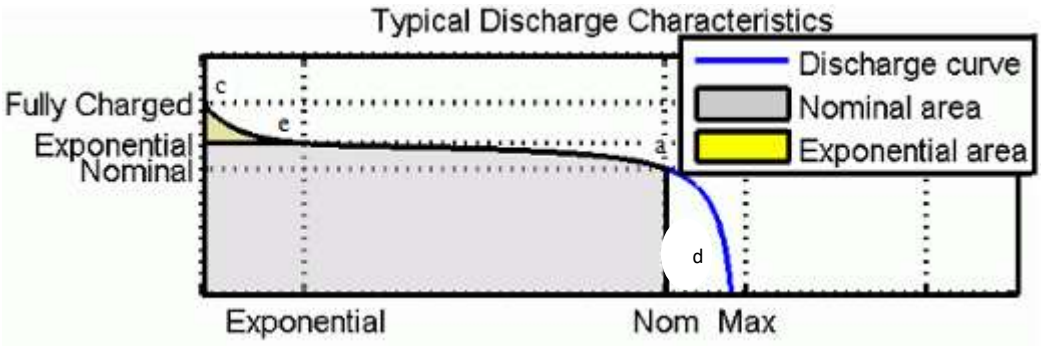

Figure 2-7 :Discharge curve of a battery[11]

- **The exponential zone [c–e]**:(100% - 90%) is a narrow region that indicates when the battery is fully charged.
- **The linear zone [e–a]** : (90% – 20%) It is the normal and desired operating range of the battery.
- **The logarithmic zone[a-d]**: (20% - 0%) where the battery is at risk of discharging rapidly.

2.2.3 Internal Resistance Model (Ohmic Model):

It is a simplified representation of a power source, such as a battery or a cell, that includes its internal resistance (Ri), which is one of the key parameters for determining the actual state of electrochemical storage systems (ESS). This resistance plays a crucial role in estimating the operating capability of conventional vehicles, the available energy in modern hybrid and

electric vehicles, and in assessing key indicators such as State of Health (SoH) and State of Function (SoF).[12]

The model consists of an ideal voltage source connected in series with an internal resistance (Ri). This configuration captures the immediate voltage drop under load but ignores transient dynamics. It is used to estimate the basic performance of the battery in a fast and simple manner.

The DIRM is advantageous for its balance between model fidelity and computational efficiency, making it suitable for real-time applications such as battery management systems (BMS).

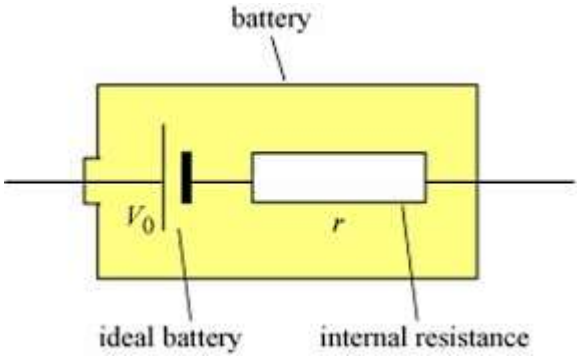

Figure 2-8 : Battery with Internal Resistance Model[12]

2.2.4 Dynamic Internal Resistance Model (DIRM):

One prominent model is the Dynamic Internal Resistance Model (DIRM), which takes into account changes in a battery's internal resistance due to factors such as temperature, state of charge (SoC), and state of health (SoH).

In a study titled "Dynamic Internal Resistance Modeling and Thermal Characteristics of Lithium-ion Batteries for Electric Vehicles by Considering State of Health," a combined thermal-electrical model based on DIRM was developed to simulate battery behavior more accurately. This model enables prediction of battery temperature rise and its effects on electrical performance, helping improve the design of battery management systems in electric vehicles.[11]

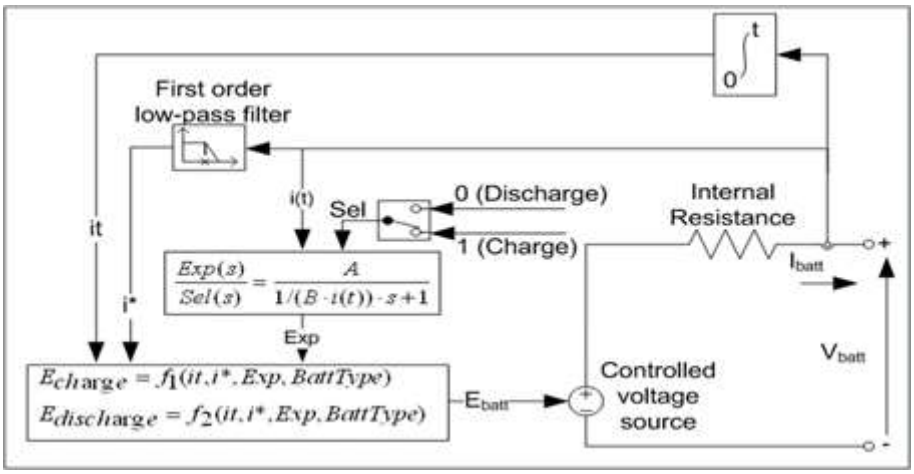

Figure 2-9 :Battery block representation as a generic dynamic model.[20]

The DIRM conceptualizes the battery as an equivalent circuit comprising:

- An open-circuit voltage source VOC (SoC) which depends on the state of charge (SoC).
- An ohmic resistance R0 , representing the instantaneous voltage drop due to internal resistance.
- One or more RC (resistor-capacitor) parallel networks (Ri,Ci), capturing the transient voltage behavior.

The terminal voltage V(t) of the battery can be expressed as:

$$V(t) = Voc(SoC(t)) - R_0 \cdot I(t) - \sum_{i=1}^{n} Vc_i\,(t) \qquad \text{(II.10)}$$

Where :

- Voc (SoC(t)) : Open-circuit voltage as a function of SoC at time t.
- R_0 : Ohmic internal resistance.
- I(t) : Current at time t (positive for discharge, negative for charge).
- $VC_i(t)$: Voltage across the capacitor C_i in the i-th RC network.
- n: Number of RC networks used to model the transient behavior.

2.2.5 General Nonlinear (GNL) Model :

The General Nonlinear Model (GNL) is an advanced model for representing battery behavior, particularly lithium-ion batteries. It is used to model the nonlinear relationships between

voltage, current, temperature, and state of charge (SOC). It is widely adopted in complex systems that require high accuracy in estimation and control, such as Battery Management Systems (BMS) in electric vehicles and drones.[2]

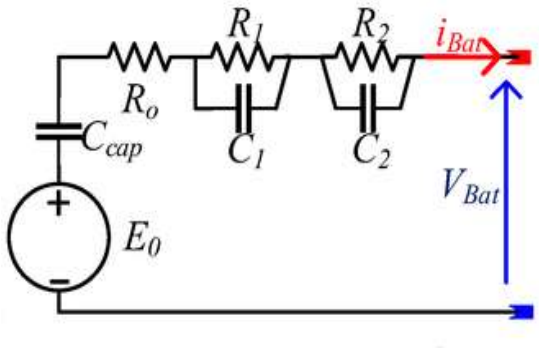

Figure 2-10 :General Nonlinear (GNL) Model [2]

The basic equation:

$$V_{bat} = OCV(SOC) - I.R(SOC, T, I) - f_{nonlinear}(SOC, I, T) \quad \text{(II.11)}$$

Vbat: Battery terminal voltage the actual voltage measured across the battery terminals under operation.

OCV(SOC): Open Circuit Voltage the voltage of the battery when no current is flowing. It depends on the State of Charge (SOC) of the battery.

I: Current positive during discharge, negative during charging.

R(SOC,T,I): Internal resistance of the battery varies with the State of Charge (SOC), temperature (T), and current.

$\mathbf{f_{nonlinear}(SOC, I, T)}$ **:** Nonlinear effects , this term accounts for complex electrochemical behaviors such as:

- Polarization
- Ion transport limitations
- Dynamic capacity effects
- Other nonlinear chemical phenomena

The GNL model can be constructed in one of two ways:

- **Experimental Data Approach**: Using Lookup tables, voltage-current-SOC data is collected under different conditions.
- **Machine Learning Approach**: Neural networks or optimization algorithms are used to generate dynamic approximation functions.

These models are used to simulate battery performance under various scenarios with the ability to accurately predict its behavior.

2.2.6 Single Particle Model (SPM) :

The Single Particle Model (SPM) is a widely used reduced-order model in Battery Management Systems (BMS) for estimating internal states such as State of Charge (SOC) and State of Health (SOH). It is derived from the full-order electrochemical model of the battery and thus retains some of its essential physical characteristics. The SPM assumes that each electrode consists of a single spherical particle representing the aggregate be havior of the electrode, with a uniform current distribution across both electrodes and a spatially and temporally constant electrolyte concentration. Due to its relative simplicity compared to full-order models, the SPM is well-suited for real-time estimation and control applications, and has served as a foundation for developing Kalman filters and adaptive observers for accurate battery state estimation.[14]

Figure 2-11 portrays the concept of the SPM. In the full order electrochemical model , lithium ion transports in the solid and electrolyte phase. The key idea of the SPM is that the solid phase of each electrode can be modeled as a single spherical particle, and lithium ion concentration in electrolyte phase is assumed to be constant in space and time.The SPM specifically does not include mechanical responses, whose effect on diffusion becomes significant when the material has high modulus and high partial molar volume .[14]

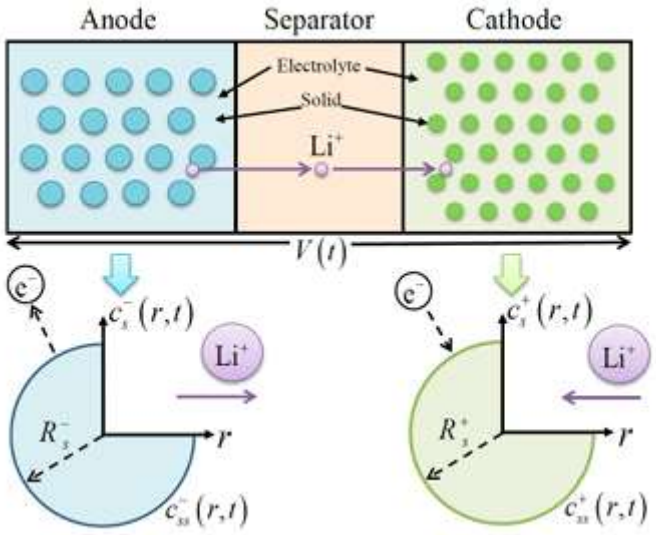

Figure 2-11 :Sketch of the Single Particle Model concept.[14]

For the case of a spherical particle, the intercalation of lithium ions in the solid phase is modelled as a process due to diffusion and stress generation, given by: [16]

$$\frac{\partial c_s^j}{\partial t} = D_s^j \left[\frac{\partial^2 c_s^j}{\partial r^2} - \frac{\Omega^j}{RT} \frac{\partial c_s^j}{\partial r} \frac{\partial \sigma_h^j}{\partial r} - \frac{\Omega^j c_s^j}{RT} \left(\frac{\partial^2 \sigma_h^j}{\partial r^2} + \frac{2}{r} \frac{\partial \sigma_h^j}{\partial r} \right) \right] \qquad \text{(II.12)}$$

∂c_s^j : Lithium concentration in the solid particle of electrode j (mol/m³)

D_s^j: Solid-phase diffusion coefficient for electrode

Ω^j: Partial molar volume of lithium in the material

- ✓ **Advantages:**
  - + **Mathematical Simplicity:** The model is significantly simpler than full-order electrochemical models, making it suitable for analysis and real-time applications.
  - + **Computational Efficiency:** Requires fewer computational resources, making it ideal for embedded use in Battery Management Systems (BMS).

+ **Preserves Key Physical Characteristics:** Despite its simplicity, SPM retains essential features of lithium transport within solid particles.

+ **Reasonable Accuracy for SOC/SOH Estimation:** Proven effective when combined with estimation techniques such as Kalman Filters or adaptive observers.

+ **Extendable Framework:** Can be extended to include additional effects such as mechanical stress or electrolyte dynamics.

✓ **Disadvantages:**

- **Neglects Electrolyte Dynamics:** Assumes constant electrolyte concentration, which limits accuracy under high dynamic conditions like high C-rates.

- **Excludes Mechanical Effects:** Does not account for mechanical stress or particle expansion, which are important for battery aging and safety.

- **Idealized Assumptions:** Assumes each electrode is a single particle, ignoring spatial variations in lithium concentration and current density.

- **Limited Accuracy in Demanding Applications:** May not be sufficient for industrial or high-precision applications requiring detailed voltage predictions.

2.2.7 Randles Circuit Model :

The Randles Circuit Model is an equivalent electrical circuit used to represent the electrochemical response of a cell in Electrochemical Impedance Spectroscopy (EIS) analysis. This model consists of the solution resistance (Rs), the double-layer capacitance (Cdl), the charge transfer resistance (Rct), and the Warburg element (Zw), which represents the ionic diffusion process , as shown in the figure2-12.

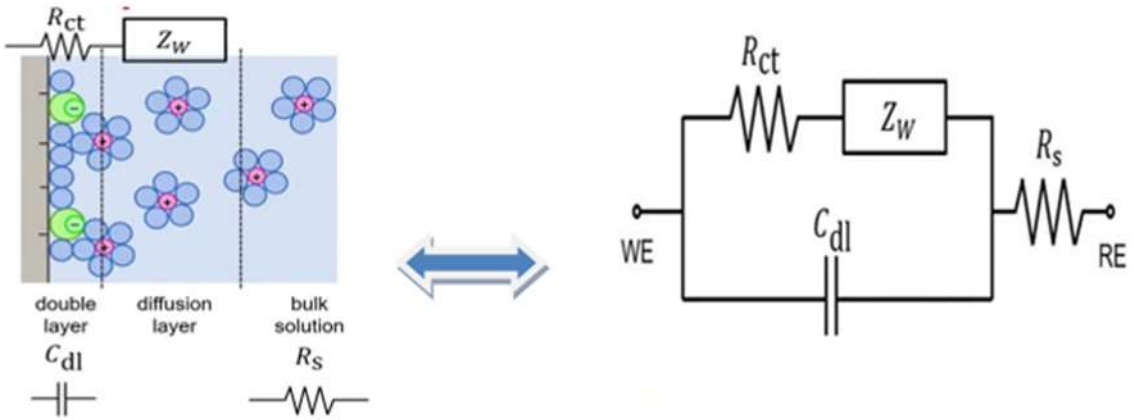

Figure 2-12 :Equivalent Randles Circuit Model.[13]

Solution Resistance (Rs):

Represents the resistance of the electrolyte (also known as the ohmic resistance).

Double-Layer Capacitance (Cdl):

Represents the electric double layer formed at the electrode/electrolyte interface.

Charge Transfer Resistance (Rct):

Represents the resistance that hinders the charge transfer reaction at the interface.

Warburg Impedance (Zw):

Represents the ionic diffusion process within the electrolyte and the electrode.

This model is widely used in the study of batteries, fuel cells, and electrochemical solar cells, as it provides a simplified physical understanding of charge transfer processes, ion accumulation, and interfacial reactions between the electrodes and the electrolyte. Due to its simplicity and the physical interpretability of its components, the Randles model is considered a fundamental tool for evaluating the performance of electrochemical materials.

- ✓ **Advantages:**

  - + Simple and widely used model.
  - + Useful for analyzing EIS data.
  - + Model parameters have physical significance.
  - + Suitable for low and medium frequency ranges.

✓ **Disadvantages:**

- Assumes linearity and time invariance.
- Not suitable for analyzing fast charge/discharge (high C-rate) or transient conditions.
- Overly simplified for complex systems such as lithium-ion batteries with nonlinear behavior.

2.3 Comparison Between Equivalent Models:

Each scheme has its own strengths and limitations, depending on the Typical Applications and the level of Complexity and Accuracy, they are described in the next table:

Model	Complexity Level	Accuracy	Typical Applications
Thevenin Model (Single RC)	Low	Good	Basic control applications (e.g., BMS)
Thevenin Model (Dual RC)	Medium	Very Good	Improved voltage prediction and load behavior
Ideal Voltage Source Model	Very simple	Very low	Theoretical analysis only
Internal Resistance Model (Ohmic Model)	Simple	Low to Medium	Fast simulation, basic understanding
Dynamic Internal Resistance Model (DIRM)	Medium to High	Very Good	Enhanced dynamic behavior modeling under load
General Nonlinear (GNL) Model	High	High	Advanced studies, long-term prediction
Single Particle Model (SPM)	Very High	High	Detailed chemical simulation of Li-ion cells
Randles Circuit Model	Medium	Good	Electrochemical Impedance Spectroscopy (EIS) analysis
Electrochemical Model	Very high	Excellent	Research, thermal modeling

Table 8 :Comparison Between Equivalent Models

2.4 Battery Performance Indicators:

2.4.1 State of charge (SOC):

State of Charge **(SoC**) is defined as the percentage of the remaining battery capacity relative to its maximum capacity. Two of the most common and straightforward methods for estimating SoC without relying on physical models are the Kalman Filter and Coulomb Counting. [16]

However, the accuracy of **SoC** estimation is influenced by several operational and environmental factors, including temperature, charging/discharging currents, battery aging, and changes in effective capacity due to cycling. As a result, accurately estimating SoC presents a significant technical challenge, requiring the use of advanced algorithms based on mathematical modeling or artificial intelligence techniques, such as extended Kalman filters and artificial neural networks.

SoC estimation is a fundamental function in Battery Management Systems (**BMS**s). It supports informed decision-making regarding system operation, prevents overcharging and deep discharging, thereby extending battery life and enhancing system safety.

This estimation becomes even more critical in sensitive applications such as electric vehicles (**EVs**), unmanned aerial vehicles (**UAVs**), and renewable energy storage systems, where overall system performance heavily depends on the accuracy of **SoC** determination. Inaccurate estimations can lead to decreased reliability and efficiency, or even pose serious safety risks , SoC is defined as:

$$SOC(t) = \frac{Q_{available}(t)}{Q_{nominal}} \times 100\% \qquad \text{(II.13)}$$

$\mathbf{SOC(t)}$ **:** State of charge at time t (in percentage %).

$\mathbf{Q_{available}(t)}$ **:** the amount of remaining electric charge in the battery at time t, in ampere-hours (Ah)**.**

$\mathbf{Q_{nominal}}$ **:** the nominal full charge capacity of the battery, also in ampere-hours (Ah).

Or SoC estimation with a CC method :

$$SOC(t)\% = SOC(0) - \frac{1}{Q_N}\int_0^t I_b(t)dt \times 100 \quad \text{(II.14)}$$

2.4.2 State of health (SOH):

Batteries degrade over time due to chemical and mechanical processes, resulting in reduced capacity, power capability, and safety. To ensure optimal usage and predict failure, the State of Health (SOH) provides a quantitative indicator of battery aging. SOH is typically expressed as a percentage, where 100% represents the battery's state when new.[16]

The phenomenon of the gradual decline in battery capacity over time and with frequent use is partly due to unwanted side reactions that consume the available lithium ions, in addition to the degradation of the electrodes, leading to what is known as capacity fade as illustrated in Figure 2-13.

Although there are several methods for estimating the battery's State of Health (SOH), some of these methods require lengthy and complex testing procedures, which makes them unsuitable for applications that require real-time or operational estimation.

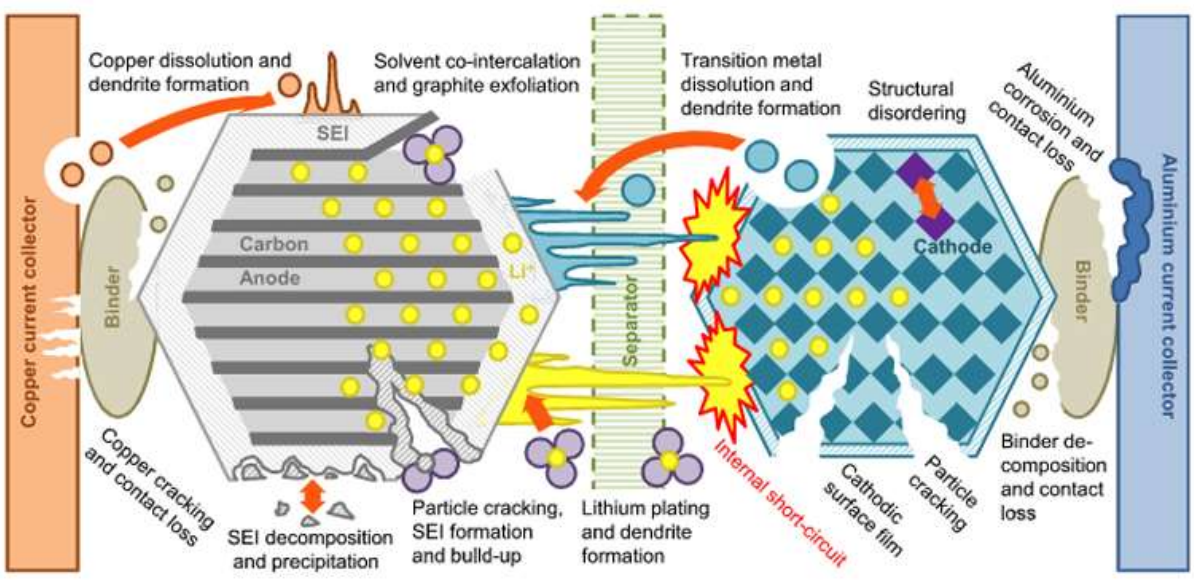

Figure 2-13 :Different ways a battery can degrade[3]

SOH can be defined in several ways depending on the application, but most commonly it is calculated as:

$$\mathrm{SOH}(\%) = \frac{\mathrm{C_{actual}}}{\mathrm{C_{nominal}}} \times 100 \quad \text{(II.15)}$$

Where:

- $\mathbf{C_{actual}}$**:** Current usable capacity of the battery
- $\mathbf{C_{nominal}}$: Rated (nominal) capacity when the battery was new

In some cases, internal resistance or maximum power capability are also used as SOH indicators.

✓ **SoH approximation from cycle counting :**

State of Health (SoH) estimation using cycle counting relies on tracking the number of charge-discharge cycles the battery undergoes. Each full charge cycle gradually leads to capacity degradation over time. This approach assumes that the battery loses a specific percentage of its capacity after a certain number of cycles, represented by the capacity fade curve (Figure 2-14). Consequently, SoH can be estimated by comparing the number of completed cycles with the expected end-of-life cycle count, typically when the battery reaches 80% of its original capacity. Despite the simplicity and low cost of this method, it does not consider other influencing factors such as temperature or depth of discharge, which may affect the accuracy of the estimation.

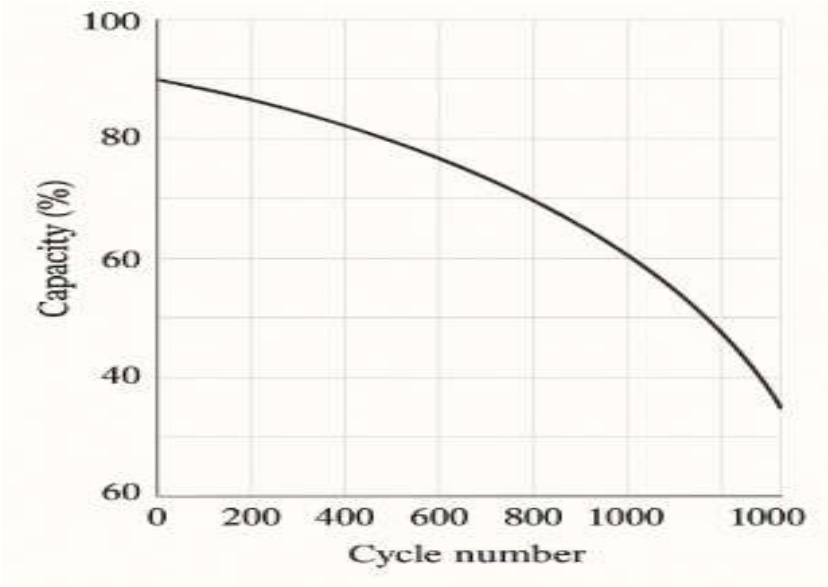

Figure 2-14 : The capacity fade curve[3]

To calculate the SoH using cycle number counting, the equation used is shown below:

$$SOH = \frac{N_{total} - N_{exp}}{N_{total}} \quad \text{(II.16)}$$

✓ **Importance of Estimating Battery State of Health (SOH):**

Safety Assurance	Accurate SOH estimation helps prevent risks associated with damaged or degraded cells, such as explosions or overheating.
Predictive Maintenance	Enables proactive maintenance instead of reactive repairs, reducing operational costs and improving system uptime.
Performance Optimization	Facilitates monitoring of battery performance over time and allows adjustments to charging/discharging strategies.
Extended Battery Life	Improved load and cycle management helps slow down degradation and extend the battery's serviceable life.
Warranty Verification	Acts as an objective measure to verify whether a battery still meets warranty criteria for both users and manufacturers.
Efficient Energy Management	Supports better overall energy efficiency, particularly in systems that heavily rely on batteries.
Crucial for Critical Applications	Essential in applications like EVs, solar systems, medical devices, and drones where reliability depends on battery health.
Supports Research and Development	SOH is a core parameter in battery research and predictive modeling, driving innovation in energy storage technologies.

Table 9 :Importance of Estimating Battery State of Health (SOH).

2.4.3 Depth of discharge definition (DOD):

Depth of discharge (DoD) is how much the battery has been discharged com pared to its full capacity. Most BMS limit the DoD to 80%. This implies that with a battery of 100Ah with a DoD of 80%, the battery has been discharged with 80Ah. The DoD is usually stated at 90% SoC until 20%. The useful ca pacity is the capacity that can be extracted from the battery.

When a battery of a capacity of 100 Ah is discharged at a DoD of 80%, which the BMS limits, the capacity is measured or estimated.[3]

The measured or estimated extracted capacity is the useful capacity.

To calculate the Depth of Discharge (DoD) of a battery, the following equation can be used:

With **SOC** :

$$\mathrm{DOD\%} = 1 - \mathrm{SOC\%} \tag{II.17}$$

Or without **SOC**:

$$DOD\% = \left(\frac{\text{(la capacité rétiré d'une batterie chargé (Ah)}}{\text{Cn(Ah)}}\right) \tag{II. 18}$$

2.4.4 End of Life (EOL):

The End of Life (EoL) of a battery refers to the stage at which the battery can no longer perform its intended functions within the defined technical specifications. This concept is crucial in battery management systems, as it helps determine the appropriate time for battery replacement or retirement. Typically, EoL is defined when the battery's capacity drops to 80% of its original nominal capacity, meaning it is no longer able to store the same amount of energy as it did when new. This gradual decrease in capacity is known as capacity fade, which occurs naturally due to repeated charging and discharging cycles, as well as environmental factors such as high temperatures. [3]

2.4.5 State of Function (SOF):

State of Function or State of Functionality, this is a term sometimes used in Battery Management Systems (**BMS**) or in other contexts to represent the system's or device's ability to perform its intended function under current conditions. However, **SOF** is not as commonly used as **SoC** (State of Charge) or **SoH** (State of Health).[3]

2.5 Different techniques used to quantify the SOC:

2.5.1 Battery Voltage Method (Open Circuit Voltage - OCV):

The Open Circuit Voltage (OCV) method is a non-invasive technique for estimating the State of Charge (SoC) of electrochemical batteries by correlating the battery's terminal voltage at rest with its SoC. The OCV is a function of the internal electrochemical potential, which varies predictably with the amount of charge stored in the cell. This relationship is typically characterized experimentally and used to map measured OCV values to SoC levels.

When the open-circuit voltage (OCV) is known, the State of Charge (SoC) can be estimated using an inverse function:

$$f^{-1}(ocv) = SOC \tag{II.19}$$

where:

f^{-1} is the inverse function of the OCV-SoC curve, which is determined experimentally.

2.5.1.1 OCV-SoC Curve:

The OCV-SoC curve is typically nonlinear and often takes the shape of a **logistic** or **polynomial** function.

Example of an approximate polynomial function:

$$V_{oc\_th}\,(soc) = P_1 \times SOC^{10} + \times P_2\, SOC^9 + P_3 \times SOC^8 + P_4 \times SOC^7 + P_5 \times SOC^6 + P_6 \times SOC^5 + P_7 \times SOC^4 + P_8 \times SOC^3 + P_9 \times SOC^2 + P_{10} \times SOC^1 + P_{11} \tag{II.20}$$

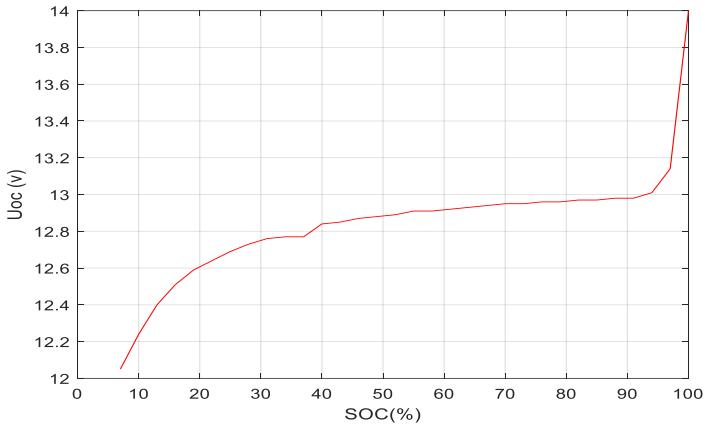

Figure 2-15 :The open circuit voltage (OCV) and the state of charge (SOC) for a lithium-ion battery

- On the left (0% SOC), the voltage is low (~3.0 V).
- As the battery charges, the voltage gradually increases.
- At 100% SOC, the voltage reaches approximately 4.2 V.

This type of curve is used in Battery Management Systems (BMS) to accurately estimate SOC during rest periods.

2.5.2 The Recursive Least Squares (RLS)

The Recursive Least Squares (RLS) algorithm is an advanced adaptive method used to estimate parameters in time-varying systems. It is characterized by its ability to update parameters immediately with each new measurement. This method has proven effective in many applications, particularly in Battery Management Systems (BMS) for accurately estimating the State of Charge (SoC) in real-time.

2.5.2.1 Principle of Operation:

The RLS algorithm works by minimizing the cumulative error between the measured values and the predicted values of the system, through iterative adjustment of the model parameters. In the context of batteries, RLS can be used either:

- To estimate the physical parameters of the battery model (such as internal resistance or the open-circuit voltage curve OCV-SoC),
- Or to estimate the State of Charge (SoC) itself, if it is included in a simplified mathematical model.

Where equation :

$$\hat{y} = \phi^T(k).\hat{\Theta}(k) \tag{II.21}$$

y(k): the measured terminal voltage of the battery.

ϕ(k): the input vector (includes current, voltage, or SoC).

$$e(k) = V_b(k) - \phi^T(k).\hat{\Theta}(k-1) \tag{II.22}$$

Gain Calculation:

$$K(k) = \frac{P(k-1)\phi^T(k)}{\lambda + P(k-1)\phi^T(k)} \tag{II. 23}$$

Covariance Matrix Update:

$$P(k) = \frac{P(k+1) - K(k)\phi(k)P(k-1)}{\lambda} \tag{II. 24}$$

λ: the forgetting factor**,** typically close to 1, to ensure numerical stability and give more weight to recent measurements.

2.5.2.2 Advantages of the Recursive Least Squares (RLS) Algorithm:

Advantage	Description
Real-time updating	RLS updates parameters immediately with each new data sample, making it ideal for real-time use.
High accuracy	By minimizing cumulative error, RLS achieves higher estimation accuracy compared to methods like LMS.
Ability to track system changes	It can adapt to time-varying system properties, such as battery degradation or dynamic behavior.
Suitable for non-stationary systems	Well-suited for systems whose characteristics change over time, like batteries under different loads.
Applicable to physical model parameters	Can be used to estimate physical parameters such as battery resistance or the OCV-SoC curve.
Mathematical stability	With proper selection of the forgetting factor λ\lambda, RLS ensures numerical stability.
Acceptable computational efficiency	Though more complex than simpler methods, it's still implementable on embedded control units (MCUs).

Table 10 :Advantages of the Recursive Least Squares (RLS) Algorithm

2.5.3 Coulomb Counting Method:

The Coulomb Counting Method, also known as the current integration method, is based on calculating the amount of electric charge entering the battery during charging and exiting during discharging by integrating the current over time. The accuracy of this method largely depends on the precision of the current sensor, the timing of the integration, and the coulombic efficiency, which varies according to the battery's condition and operating environment. Despite its simplicity and ease of implementation, one of its main drawbacks is that it does not account for the battery's self-discharge phenomenon. Moreover, any error in determining the initial State of Charge (SoC) can lead to accumulated inaccuracies over time. The method only provides relative changes in charge and lacks a mechanism for correcting drift caused by measurement inaccuracies. Nevertheless, it remains effective and suitable for systems that require real-time and continuous SoC estimation, such as electric vehicles, solar energy systems, and portable electronics—especially when simplicity and low cost are key factors in the system design., The charge's state of the battery estimation based on this method is as following:[15]

when defining the initial state of charge $SOC(0)$ and the nominal capacity C_N:

$$SOC(t)\% = SOC(0) - \frac{1}{C_N}\int_0^t I_b(t)dt \times 100 \qquad \text{(II. 25)}$$

In fig 2-16 an SoC estimation with a CC method in an environment of low noise (measurement and stable battery conditions) and severe noise (inaccurate measurement and variation of battery conditions) is shown:

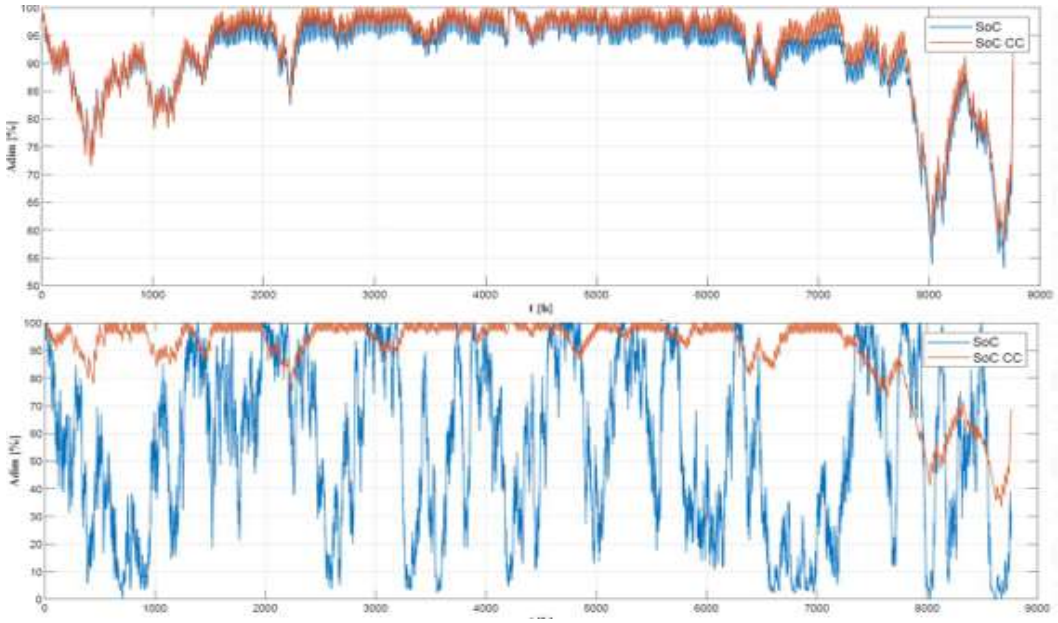

Figure 2-16 :SoC estimations by CC method for low and severe measuring errors[22]

The first case in Fig 2-16, with the estimation of CC in low error conditions, shows an average difference between the real and the estimated value of 2 %. That difference becomes much greater when non linearities such as temperature or depth of discharge (**DoD**) in the battery are included in the simulation.[22]

2.5.3.1 Coulombic Efficiency and Its Impact:

Coulombic efficiency is defined as the ratio of the charge extracted from the battery during discharge to the charge supplied during charging**,** If the efficiency is $\eta < 100\%$ meaning some of the charge is lost within the battery then using simple current integration will overestimate the actual stored charge.

correct this, it's necessary to either include the charging and discharging efficiency factors (ηc and ηd) in the equations or adjust the results obtained from Coulomb Counting accordingly.

In practice, the method often assumes $\eta=1$ as a simplified case, but many technical sources emphasize the importance of considering losses and self-discharge to maintain accurate state of charge (SOC) estimation.

2.5.3.2 Advantages of Coulomb Counting Method:

- **Ease of Implementation**: It is relatively simple in principle and can be easily implemented using microcontrollers and current sensors.
- **Low Cost**: It does not require complex equipment or advanced techniques like spectroscopy or detailed battery models, making it suitable for low-cost systems.
- **High Accuracy in the Short Term**: When using accurate current sensors and proper calibration, it can provide precise results over short time periods.
- **Not Directly Affected by Temperature**: Unlike some other methods (such as Open Circuit Voltage – OCV), this method's measurements are not directly influenced by ambient temperature.
- **Suitable for Systems That Cannot Be Shut Down**: It does not require system shutdown or rest periods for the battery, making it ideal for continuously operating systems (e.g., electric vehicles).
- **Real-Time Tracking**: It allows for real-time monitoring of the state of charge during operation without waiting for voltage stabilization or current interruption.

2.5.3.3 Challenges in the Coulomb Counting Method:

- **Error Accumulation:** Measurement inaccuracies and physical effects (such as temperature and load) lead to increasing drift in charge estimation over time.
- **Initial State Dependency:** The accuracy depends on correctly knowing or assuming the initial state of charge SOC(0): otherwise , a constant offset occurs.
- **Capacity Degradation (SOH):** Battery capacity decreases with aging, and without updating the nominal capacity , the system will overestimate the remaining charge.

- **Self-Discharge:** Batteries lose charge over time even when idle, and this loss is hard to measure precisely, increasing uncertainty in SOC estimation.

2.5.4 Kalman Filter Method:

The Kalman Filter is considered one of the most prominent mathematical tools used for estimating unknown variables in dynamic systems, such as the battery State of Charge (SoC). This filter works by integrating information derived from the system's mathematical model with real sensor measurements (such as current and voltage), making it highly suitable for Battery Management System (BMS) applications. The Kalman Filter predicts the upcoming SoC value based on the dynamic model of the battery, then corrects this estimate using voltage or current measurements. This iterative update provides accurate estimation even in the presence of measurement noise.

In a study titled *"State of Charge Estimation Using Extended Kalman Filters for Battery Management System"* conducted by Carlo Taborelli and Simona Onori, an Extended Kalman Filter (**EKF**) was developed to estimate the SoC of a lithium-ion battery used in electric bicycles[18]. The results showed that this filter provides accurate SoC estimation even under dynamic operating conditions, while reducing the impact of measurement noise.

2.5.4.1 State Model:

Represents the evolution of the state (SoC) over time:

$$X(k) = A\,.X(k-1) + B.U(k) + w(k) \qquad \text{(II.26)}$$

$X(k)$: system state at time k(represents SoC).

A: state transition matrix .

B: input matrix (converts input current effect on SoC).

U(k): input current (charging or discharging current).

$w(k)$: process noise, modeling inaccuracies in the system model.

2.5.4.2 Measurement Model:

$$\boldsymbol{y = H\,.\,x + v} \quad \text{(II. 27)}$$

y : measurement (e.g., battery terminal voltage).

C : observation matrix (relates state to measurement).

v : measurement noise.

2.5.4.3 Kalman Filter Steps

- **Prediction Step:** It is the step in which the prior estimate of the system state (such as the battery State of Charge – SoC) is corrected using actual measurements obtained (such as the measured battery voltage).

  Predict the state:

$$\hat{x}_k = A.\hat{x}_{k-1} + B.u_k \quad \text{(II. 28)}$$

  Predict the error covariance:

$$P_k = A.P_{k-1}.A^T + Q \quad \text{(II.29)}$$

  Q : is the covariance matrix of the process noise

- **Update (Correction) Step:**

- Calculate Kalman gain:

$$K_k = P_{k-1}.H^T(H.P_{k-1}.H^T + R)^{-1} \quad \text{(II.30)}$$

R : is the covariance matrix of the measurement noise.

Update estimate with measurement:

$$\hat{x}_k = \hat{x}_{k-1} + K_k(y_k - H.\hat{x}_{k-1} \quad \text{(II.31)}$$

Update error covariance:

$$P_k = (I - K_k.\mathrm{H}).P_{k-1} \quad \text{(II.32)}$$

Based on the study results *(By Da-Yan Liu1, Wen Chen2 , Driss Boutat1 . 'State of Charge Estimation of Lithium-ion Batteries based on Fractional-order Modulating Functions'. Proceedings of the 2024 12th International Conference on Systems and Control, Batna, Algeria, November 03-05, 2024*) [19], fig 2-17 and fig 2-18 which are presented in the form of curves, we discuss as follows :

The red curve shows the estimation of the terminal voltage over time. We observe that the estimated terminal voltage increases gradually with increasing time. The blue curve shows the estimation of the initial value of the SoC (State of Charge). We observe that the initial value of the SoC starts around 0.1 (10%) and increases gradually over time. In general, these curves provide information on how to estimate the terminal voltage and the initial value of the SoC in an electrochemical storage system, using a Kalman filter, which indicates that the system is operating correctly.

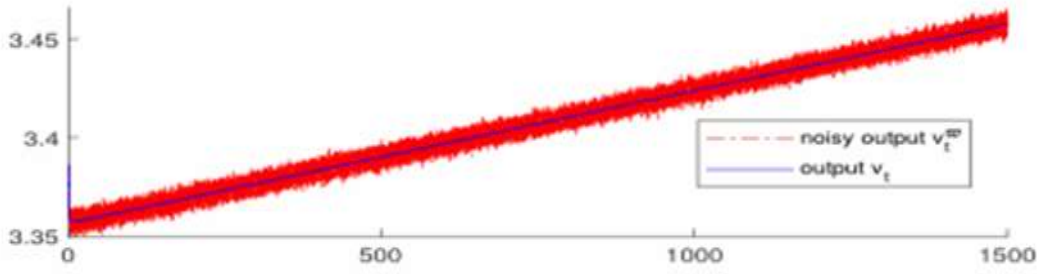

Figure 2-17 :The noisy terminal voltage, current and process noises[19]

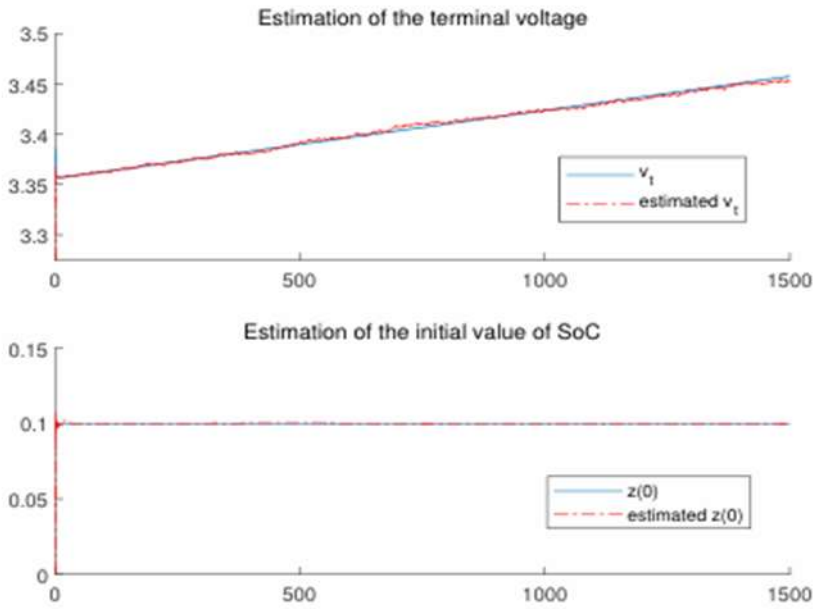

Figure 2-18:Estimations of the terminal voltage and the initial value of the SOC[19]

2.5.5 Neural networks in battery state of charge estimation:

Neural networks rely on processing input data such as voltage, current, and temperature through multiple layers of nodes (neurons), where the weights are adjusted internally during training so that the network can accurately predict the value of the SoC. Activation functions such as ReLU or Sigmoid are used to enhance learning accuracy. After training, the network becomes capable of providing real-time state estimations based on new incoming data.

$$SOC_{\text{predicted}} = f(W_2.f(W_1.X + b_1) + b_2) \quad \text{(II.33)}$$

X is the input vector (e.g., voltage, current, temperature)

W_1 W_2 are weight matrices

b_1 b_2 are bias vectors

f is a nonlinear activation function

✓ **The types of networks used in SoC estimation:**

Conventional networks (such as multi-layer networks): These are used to process static data and estimate SoC based on inputs such as voltage, current, and temperature.

Recurrent Neural Networks (RNNs) and their improved variants like LSTM: These are ideal for tracking SoC over time, as they take into account the temporal sequence of the data.

✓ **Advantages and Disadvantages :**

Advantages	Disadvantages
High Accuracy	Requires Large Training Data
Adaptable to Different Batteries	Hard to Interpret and Verify
Suitable for Nonlinear Systems	Computationally Expensive Initially
Continuously Updatable	Performance Depends on Data Quality
Real-Time Support	Risk of Overfitting

Table 11 :Advantages and Disadvantages of Neural networks

2.6 Conclusion:

This chapter presented a comprehensive overview of various modeling approaches for solar batteries using equivalent electrical circuits. The focus was placed on the Thevenin equivalent circuit and its hysteresis-enhanced variant, both of which are widely used for capturing the dynamic behavior of batteries. Additional models were briefly discussed to highlight alternative representations that consider thermal and electrochemical effects.

Key battery performance indicators State of Charge (**SoC**), State of Health (**SoH**), and Depth of Discharge (**DoD**) , were defined and explained in detail due to their critical importance in battery monitoring and lifetime estimation. Moreover, different techniques used to estimate SoC were explored, including Coulomb counting, voltage-based methods, and model-based estimators like the Kalman Filter, along with a discussion of their advantages and limitations.

Together, these models and definitions provide a solid foundation for the development of Battery Management Systems (**BMS**) in solar energy applications. Accurate battery modeling and state estimation are essential for enhancing the efficiency, safety, and longevity of systems.

Chapter III: Using three methods to estimate the state of charge. (Simulation).

3 Chapter III: Using three methods to estimate the state of charge. (Simulation).

3.1 Introduction:

In this chapter, a set of established methods for estimating the State of Charge (SoC) will be presented, with a focus on three fundamental algorithms that represent different approaches in this field:

- Recursive Least Squares (RLS)
- Coulomb Counting
- Kalman Filter

This study aims to evaluate the performance of each method through simulation models developed using the Matlab/Simulink environment. The goal is to analyze the accuracy, flexibility, and responsiveness of each method under various operating conditions that may affect the battery.

At the end of the chapter, a comprehensive comparison of the studied methods will be conducted to identify the most optimal approach for SoC estimation in terms of efficiency and accuracy, while taking into account the key factors that influence battery behavior

NOTE: In all the experiments conducted in this report and the methods used, a lithium-ion battery was studied and tested in the discharge state.

3.2 Battery parameter identification :

Such as internal resistance, capacitance, and components of the equivalent circuit model, which depend on the type of model used in this experiment a lithium-ion battery.

✓ The battery is modeled using the Thevenin model :

The equivalent circuit model chosen for the battery is the one shown in the adjacent figure 3-1, which is widely used and known as the " Thevenin model with a polarization branch"

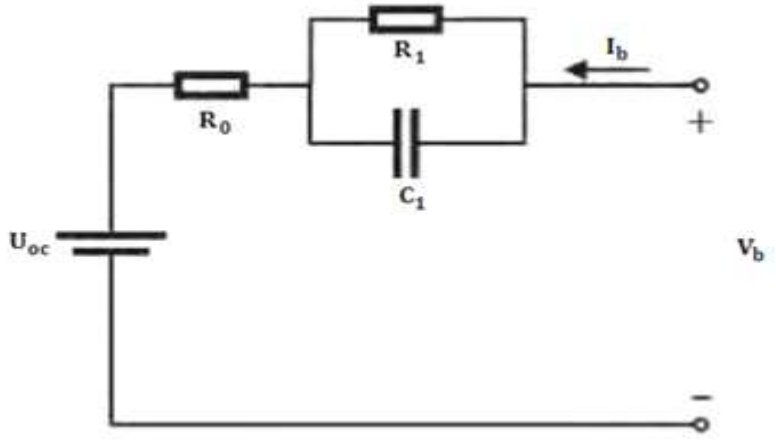

Figure 3-1 :Thevenin model with a polarization branch[21]

Where:

Uoc : Open-circuit voltage, which is a function of the state of charge SOC(t).

R0 : Resistance representing Joule losses.

(R1, C1): Polarization branch.

The model is given in the Laplace domain, with V_b and I_b , respectively:

$$V_b(S) = U_{OC}(S) - I_b\left[R_0 + \frac{R_1}{1 + R_1 C_1 s}\right] \quad \text{(III. 1)}$$

$$G_{eq}(S) = \frac{V_b(S) - V_{OC}(S)}{I_b(S)} \quad \text{(III. 2)}$$

By using the bilinear transformation:

$$S = \frac{2}{T_S}\frac{1 - z^{-1}}{1 + z^{-1}} \tag{III. 3}$$

Where:

T_s : Sampling period

Thus, the discretized transfer function is :

$$G(z^{-1}) = -\frac{\left(\frac{R_0T + R_1T + 2R_0R_1C_1}{T + 2R_1C_1} + \frac{R_0T + R_1T - 2R_0R_1C_1}{T + 2R_1C_1}z^{-1}\right)}{1 + \frac{T - 2R_1C_1}{T + 2R_1C_1}z^{-1}} \tag{III. 4}$$

where z is the discretization operator.

We define:

$$\begin{cases} a_1 = -\dfrac{T - 2R_1C_1}{T + 2R_1C_1} \\ a_2 = -\dfrac{R_0T + R_0T - 2R_0R_1C_1}{T + 2R_1C_1} \\ a_3 = -\dfrac{R_1T + R_1T - 2R_0R_1C_1}{T + 2R_1C_1} \end{cases} \tag{III. 5}$$

We then obtain :

$$V_b(k) = V_{OC}(k) + a_1[V_{OC}(k-1) - V_b(k-1)] - a_2I_b(k) - a_3I_b(k-1) \tag{III. 6}$$

The battery voltage V_b(t) is placed in a regression form:

$$V_b(k) = \Phi^T(k).\Theta(k) \tag{III. 7}$$

Where $\Phi^T(k)$ is called the regressor, and Θ(k) is the parameter vector to be identified.

$$\Theta(k) = [V_{OC}(k)\ \ a_1\ \ a_2\ \ a_3] = \begin{bmatrix} V_{OC}(k) \\ a_1 \\ a_2 \\ a_3 \end{bmatrix} = \begin{bmatrix} \Theta_1(k) \\ \Theta_2(k) \\ \Theta_3(k) \\ \Theta_4(k) \end{bmatrix} \tag{III. 8}$$

$$\Phi^T(k) = [1 \quad V_{OC}(k-1) - V_b(k-1) \quad -I_b(k) \quad -I_b(k-1)] \tag{III. 9}$$

The parameters of the equivalent circuit are then derived using:

$$R_0 = \frac{a_2 - a_3}{a_1 + 1} \quad \text{(III. 10)}$$

$$R1 = \frac{2(a_1 a_2 + a_3)}{1 - a_1^2} \quad \text{(III. 11)}$$

$$C_1 = \frac{T_s(a_1 + 1)^2}{4(a_1 a_2 + a_3)} \quad \text{(III. 12)}$$

3.3 State of Charge Estimation Methods:

3.3.1 Recursive Least Squares (RLS) Method:

The RLS algorithm has been widely used in numerous studies, with the main objective being to minimize the sum of squared differences between the measured output $y(k)$ and the estimated output from the model, denoted as $\hat{y}(k)$.

$$J = \sum_{k=1}^{n} e^2(k) \quad \text{(III. 13)}$$

$$e(k) = y(k) - \hat{y}(k) \quad \text{(III. 14)}$$

$$\hat{y} = \phi^T(k).\hat{\Theta}(k) \quad \text{(III. 15)}$$

Since the estimated output depends on the state to be obtained $\hat{\Theta}_{old}(k)$in the last equation, this variable is replaced by the value obtained at the previous time step $\hat{\Theta}_{new}(k-1)$.

In this sense, the steps of the method are as follows:

Step 01: Initialize the prediction error e(k), and the parameter vector :

$$\Theta_{old} = [0 \quad , 0 \quad , 0 \quad , 0] \quad \text{(III. 16)}$$

Step 02: For each iteration, capture $V_b(k)$, and evaluate the prediction gain $k(k)$ by:

$$e(k) = V_b(k) - \phi^T(k).\hat{\Theta}(k-1) \quad \text{(III. 17)}$$

$$K(k) = \frac{P(k-1)\phi^T(k)}{\lambda + P(k-1)\phi^T(k)} \quad \text{(III. 18)}$$

$$P(k) = \frac{P(k+1) - K(k)\phi(k)P(k-1)}{\lambda} \quad \text{(III. 19)}$$

$$\lambda = 0.999 \approx 1 \quad \text{(III. 20)}$$

Where $P(k)$ is the covariance matrix of size $(n \times n)$, and the regressor vector is given by:

$$\phi_{new} = \begin{bmatrix} 1 & (V_{oc_{old}} - V_{b_{old}}) & -I_b & -I_{b_{old}} \end{bmatrix} \quad \text{(III. 21)}$$

Note : (K-1) it means old.

(K) its means new.

Step 03: Update the parameter vector of size (1×n) by:

$$\hat{\theta}(k) = \hat{\theta}(k-1) + K(k)e(k) \quad \text{(III. 22)}$$

It is important to note that the covariance matrix must be initialized with a large value: $P_0 = \alpha.\mathrm{I}(\mathrm{n} \times \mathrm{n})$, and α is a positive constant, in order to accelerate convergence.

$$P = [n \times n] = [4 \times 4] = \begin{bmatrix} 1 & 0 & 0 & 0 \\ 0 & 1 & 0 & 0 \\ 0 & 0 & 1 & 0 \\ 0 & 0 & 0 & 1 \end{bmatrix} \quad \text{(III. 23)}$$

We chose a 4×4 covariance matrix based on the variables we have (Voc ; a1 ; a2 ; a3).

3.3.1.1 Description of the scheme used in the simulation:

In this scheme, Cn=6.5 Ah, Vb=12 V Lithium-Ion battery powering a resistive load of R=1.2 is used ,and Initial State of Charge $\mathrm{SOC}(0) = 100\%$, $\mathrm{T_s} = 10^{-7}$.

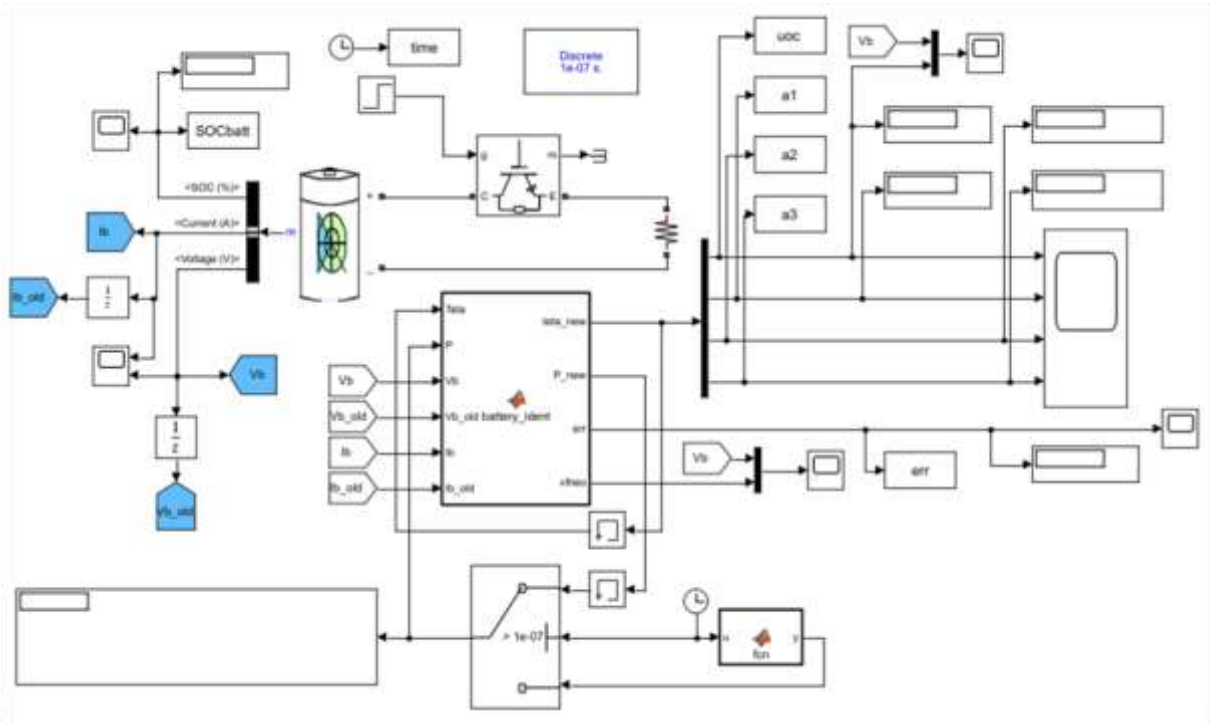

Figure 3-2: Matlab/Simulink diagram for battery testing (RLS Method)

The design of this simulation is based on the direct theory of the recursive least squares method.

The schematic shown in the previous image from Matlab/Simulink represents a battery model aimed at accurately identifying its parameters. The battery voltage V_b and the drawn current I_b are continuously measured to reflect the actual operating conditions. An Insulated Gate Bipolar Transistor (IGBT) is used to generate stepped current levels, allowing the simulation of different effects on the battery at various initial values of the state of charge SOC(t). This simulation relies on an algorithm capable of handling a wide range of SOC variations, contributing to improved accuracy in parameter estimation and more realistic battery modeling.

$0 \rightarrow 2\ s$	K = 1 (closed)
$2\ s \rightarrow 5\ s$	K = 0 (open)

Table 12 :Switching table

3.3.1.2 Simulation Results:

In this process, for each variation of the state of charge SOC(t) between $SOC_i(t)$ and $SOC_f(t)$ covering almost the entire range of SOC variation, the following results will be obtained:

SOCi (%)	100	97	94	91	88	85	82	79
SOCf (%)	99.95	96.96	93.96	90.96	87.96	84.96	81.96	78.96
Uoc (V)	14	13.14	13.01	12.98	12.98	12.97	12.97	12.96
a_1	3.472	0.005643	0.08399	0.001134	0.1567	0.01508	0.003582	0.002939
a_2	0.8243	0.02554	0.02555	0.02307	0.04167	0.03036	0.02381	0.01976
a_3	3.376	0.01014	0.09675	0.007634	0.116	0.01887	0.01022	0.0133
Err	0.02318	0.02196	0.02157	0.023	0.0223	0.02465	0.02539	0.0263
R0 (mΩ)	0.57059	0.01531	0.13351	0.015418	0.08814	0.01131	0.013541	0.006441
R1 (mΩ)	1.198027	0.020568	0.199197	0.015329	0.224452	0.038664	0.020610	0.026716
C1 (µF)	8.0149e-7	2.410e-6	2.1178e-6	32.710e-6	1.6057e-6	13.327e-6	24.433e-6	18.825e-6

SOCi (%)	76	73	70	67	64	61	58	55
SOCf (%)	75.96	72.96	69.96	66.96	63.96	60.96	57.96	54.96
Uoc (V)	12.96	12.95	12.95	12.94	12.93	12.92	12.91	12.91
a_1	0.001415	0.01051	0.06937	0.00979	0.01219	0.04841	0.01173	0.07875
a_2	0.02333	0.02216	0.01746	0.02872	0.01825	0.02436	0.03253	0.02003
a_3	0.009439	0.00152	0.0005049	0.01638	0.0004357	0.06671	0.01802	0.03948
Err	0.02724	0.00152	0.02857	0.03073	0.03179	0.03405	0.03514	0.03558
R0 (mΩ)	0.013871	0.02393	0.018218	0.012220	0.018034	0.086864	0.014341	0.021112
R1 (mΩ)	0.018944	0.003506	0.001419	0.033325	0.000426	0.131369	0.036808	0.076278
C1 (µF)	2.655e-6	1.4563e-4	1.66591e-4	1.530e-5	1.14402e-6	4.0476e-6	13.906e-6	5.5979e-6

SOCi (%)	52	49	46	43	40	37	34	31
SOCf (%)	51.96	48.96	45.96	42.96	39.96	36.96	33.96	30.96
Uoc (**V**)	12.89	12.88	12.87	12.85	12.84	12.77	12.77	12.76
a_1	0.005858	0.008866	0.02683	0.005611	0.02619	0.323	0.008414	0.003483
a_2	0.0289	0.03139	0.03549	0.02864	0.01674	0.07601	0.02602	0.03279
a_3	0.01512	0.01797	0.03592	0.005646	0.006359	0.2743	0.009875	0.01416
Err	0.03874	0.04093	0.04363	0.04576	0.0484	0.0677	0.05619	0.06096
R0 (**mΩ**)	0.013699	0.013302	0.000418	0.024360	0.023720	0.149879	0.016281	0.018695
R1 (**mΩ**)	0.030579	0.036499	0.073797	0.01097	0.013604	0.667323	0.019313	0.028091
C1 (**µF**)	16.543e-6	13.943e-6	7.1488e-6	39.242e-6	34.877e-6	1.464e-6	25.456e-6	17.675e-6

SOCi (%)	28	25	22	19	16	13	10	7
SOCf (%)	27.96	24.96	21.96	18.96	15.96	12.96	9.962	6.964
Uoc (**V**)	12.73	12.69	12.64	12.59	12.51	12.40	12.24	12.05
a_1	0.03088	0.008513	0.00579	0.02781	0.01328	0.01261	0.01567	0.2282
a_2	0.04773	0.0292	0.03526	0.02417	0.04207	0.0551	0.02655	0.006182
a_3	0.0406	0.01909	0.01562	0.008703	0.01749	0.01414	0.07778	0.1705
Err	0.06738	0.07291	0.08106	0.09024	0.1035	0.1205	0.1462	0.153
R0 (**mΩ**)	0.00691	0.010196	0.019754	0.015909	0.024910	0.041483	0.050439	0.212902
R1 (**mΩ**)	0.084228	0.037685	0.030832	0.016074	0.033868	0.026894	0.15643	0.356756
C1 (**µF**)	6.314e-6	13.043e-6	1.1507e-5	29.422e-6	14.375e-6	18.128e-6	3.298e-6	0.88071e-6

Table 13 : Identification résulte

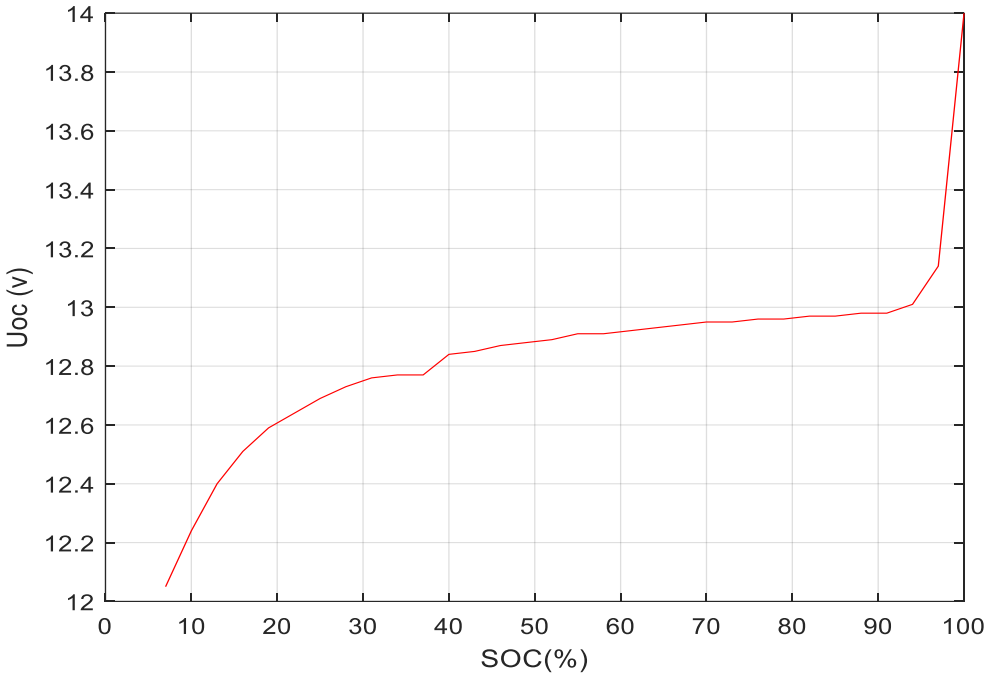

Figure 3-3 :The open-circuit voltage as a function of the state of charge.

Illustrates the behavior of the open-circuit voltage Uoc(t) as a function of the state of charge SOC(t) , with the curve divided into three main regions:

- From 9% to 40%: A logarithmic region observed at the beginning of the battery charge, generally avoided to prevent deep discharge.
- From 40% to 90%: A linear region known as the active operating range of the battery, commonly used in practical applications due to its stability and reliability.
- From 90% to 100%: An exponential region representing the fully charged state of the battery.

Knowing the state of charge is essential in many applications to ensure battery safety and performance. This estimation can be achieved either through charge equations or via the empirical relationship:

$$U_{OC}(t) = f(SOC) \qquad \text{(III. 24)}$$

In this study, the relationship was approximated using a 10th-order polynomial by applying the ‘polyfit’ function in Matlab.

V_{oc_th}=P(1)× SOC^{10} + P(2)× SOC^{9} + P(3) × SOC^{8} + P(4)× SOC^{7} + P(5)× SOC^{6}+ P(6)× SOC^{5} + P(7) × SOC^{4} + P(8)× SOC^{3} + P(9)× SOC^{2} + P(10)× SOC^{1} + P(11) (III. 25)

with :

P= [0 -1,25e^{-13} 2,728e^{-11} -3,372e^{-9} 2,596e^{-7} -1,29e^{-5} 4,147e^{-4} -8,354e^{-3} 9,744e^{-2} -5,27e^{-1} 13,031] (III. 26)

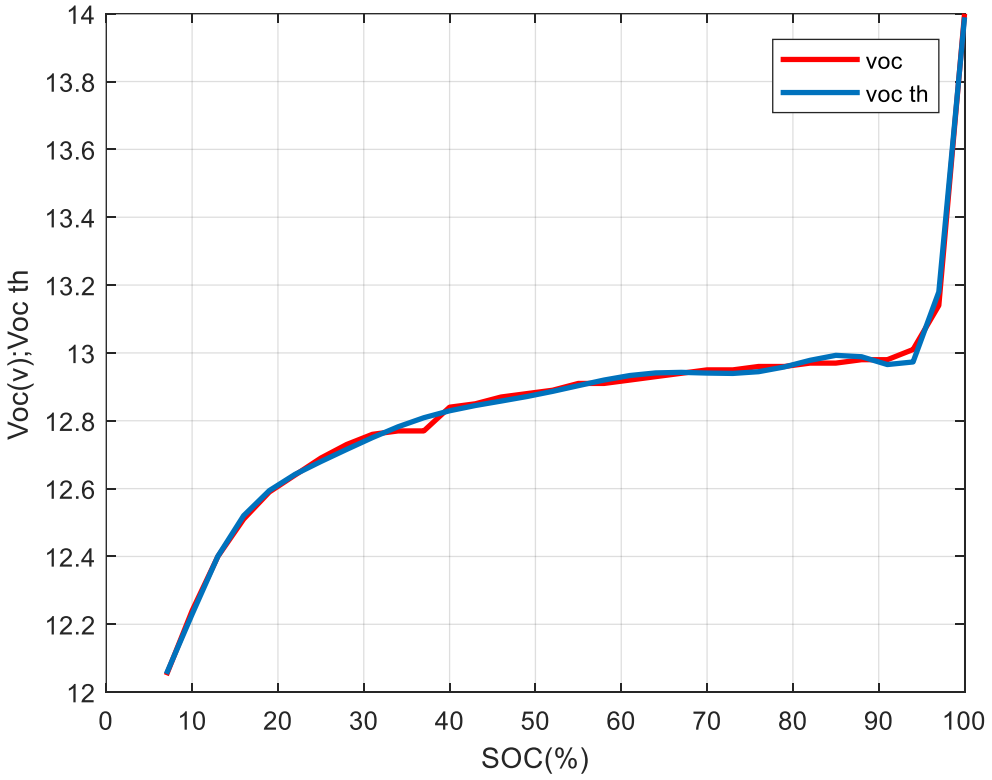

Figure 3-4 :The state of charge as a function of the open-circuit voltage

In this curve, which represents **Vocth** and **Voc** as a function of the state of charge SOC, we can observe that the curve exhibits high accuracy in predictive modeling with extremely precise alignment between **Vocth** and **Voc**.

These results were obtained using a 10th-order polynomial. This confirms the validity of the method for accurately predicting the values.

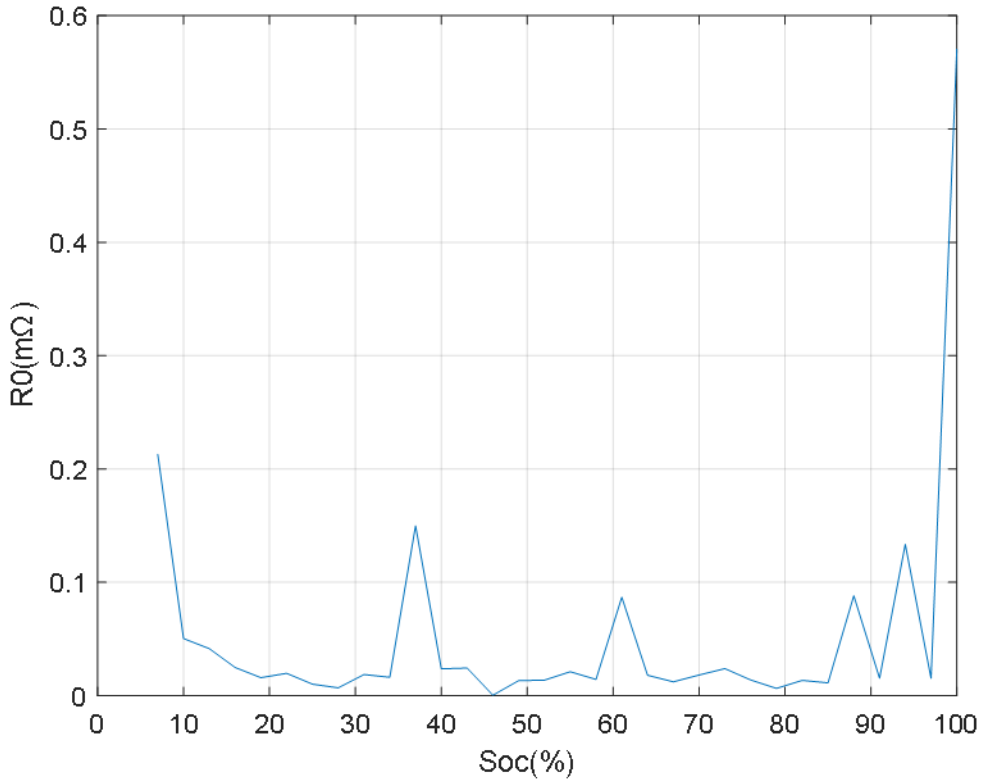

Figure 3-5 :The Joule loss resistance as a function of the state of charge.

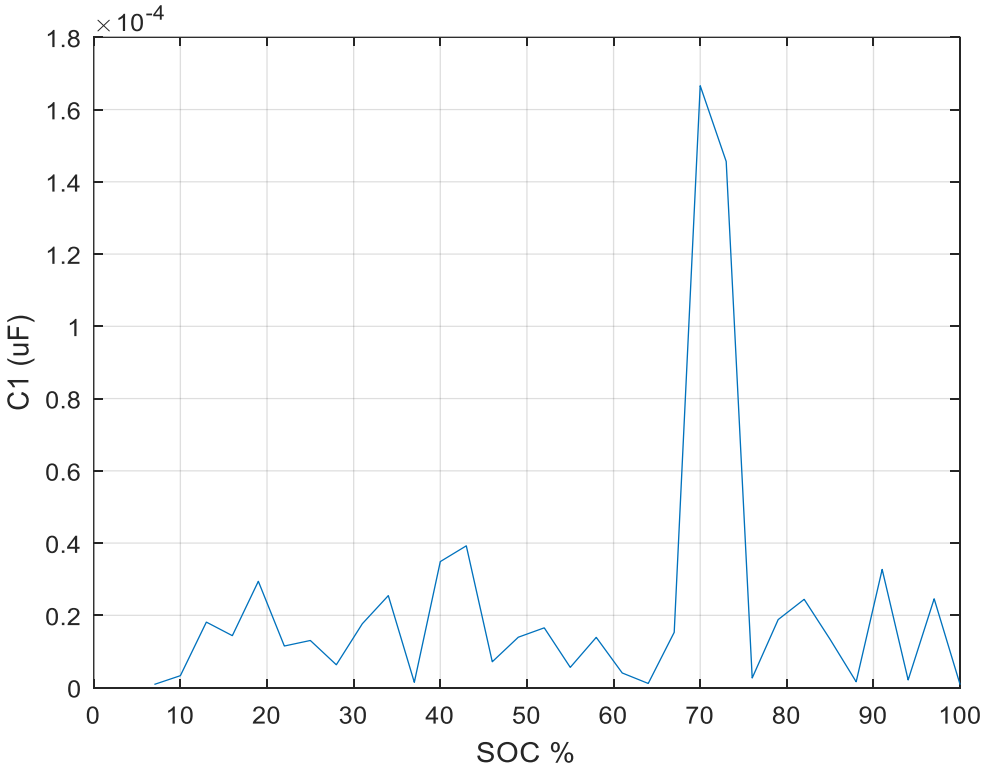

Figure 3-6 :The capacitance of the polarization branch as a function of the state of charge.

3.3.2 Coulomb based SOC algorithm:

The Coulomb Counting (CC) method is favored for its ease of implementation and effectiveness in many practical applications. This method is primarily based on measuring and accumulating the electric current flowing through the battery during charging and discharging processes, thereby calculating the amount of charge added to or withdrawn from the battery over time. By continuously integrating the current, a relatively accurate estimation of the remaining State of Charge (SOC) can be obtained, making it suitable for battery management systems that require continuous monitoring of the charge state.

However, this method requires an accurate initial SOC value to avoid error accumulation over extended periods, Its equation is as follows:

$$SOC(t) = SOC(0) - \frac{1}{C_N}\int_0^t I_b(t)dt \qquad \text{(III. 27)}$$

- SOC(0) : Initial state of charge
- C_N : Nominal capacity of the battery
- $I_b(t)$: Instantaneous current

❖ **Results of Coulomb Counting (CC) estimation method:**

To apply Coulomb's method, we use the following simulation.

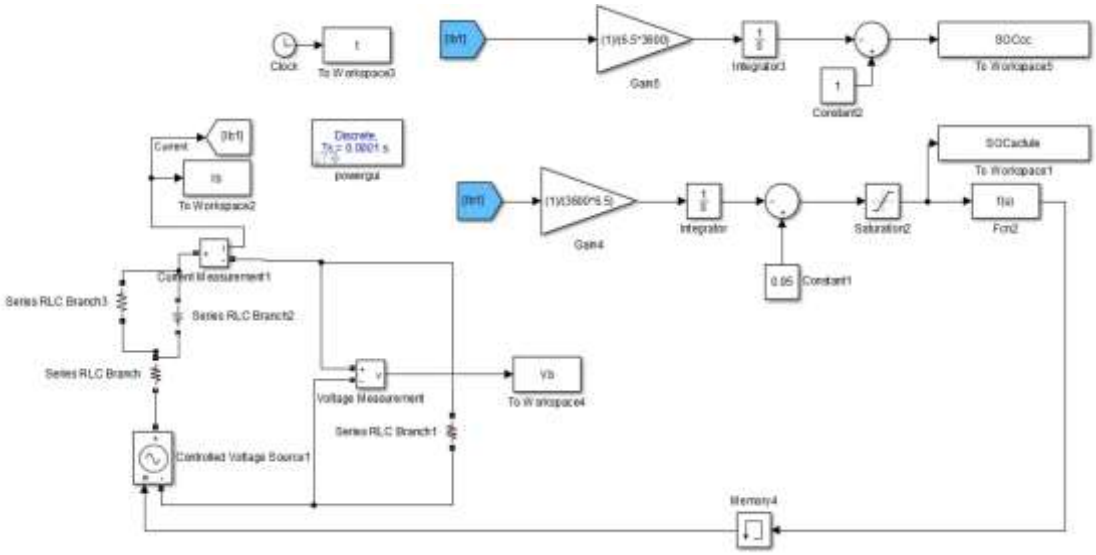

Figure 3-7 :Matlab/Simulink diagram for battery and Coulomb Counting (CC) method

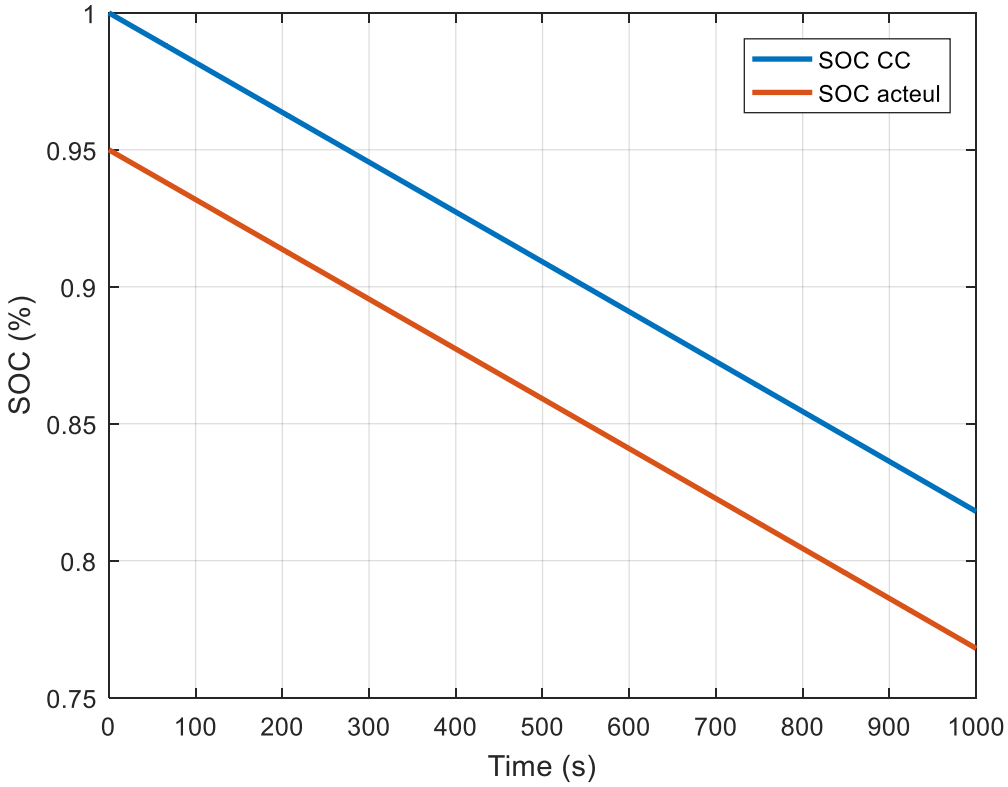

Figure 3-8 :Results of the experiment

In this simulation figure3-8,we assume that the initial value of the battery's State of Charge (SoC) using the Coulomb counting method is **100%**, while the actual SoC (**SoC_actual**) is **95%**. From the plotted curve, we observe that this slight error in the initial estimation or in the current measurement leads to a **gradual accumulation of deviation** over time.

As a result, the **Coulomb-counted SoC (SoC_cc)** curve does not approach the true value **SoC_actual**, but rather remains offset due to the initial error of **5%**. This confirms that the Coulomb counting method, when used without periodic correction or calibration, may result in inaccurate estimations of the battery's state of charge over time.

This calls for a correction of this method, which we will address in the following.

3.3.3 proposition of an adaptive law to correct it:

Given the limitations of the Coulomb counting (CC) method, an inaccurate initial state of charge (SOC) value can lead to reduced estimation accuracy, because the method does not have a correction mechanism. Moreover, since the estimation of the COS depends on the integration of the measured current over time, the accuracy of the estimation is very sensitive to the noise intrinsically present in the current measurements. To solve these problems, two adaptive methods are proposed in this thesis, the first is introduced a combined approach that integrates Coulomb Counting with Recursive Least Squares (RLS) and an Adaptive Model Reference Controller (MRAC) to correct the SOC estimation derived from the CC method. The functional diagram of the proposed solution is presented accordingly, and the second method Kalman filter based SOC estimation.:

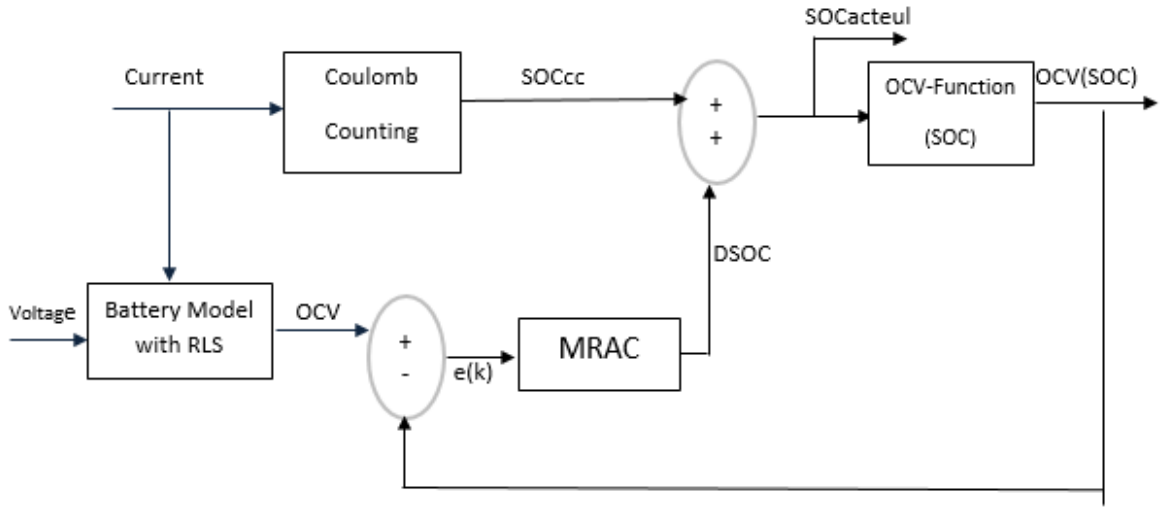

Figure 3-9 :Block diagram of the proposed method for SOC estimation[1]

In this study, Model Reference Adaptive Control (MRAC) is used to correct the State of Charge (SOC) estimation obtained from the Coulomb Counting (CC) method, with the aim of making it closely follow the ideal behavior of the battery.

- A reference model was first designed to represent the ideal variation of the State of Charge (SOC), based on actual variables such as current and voltage by this function.

$$SOC(t) = SOC(0) - \frac{1}{C_N}\int_0^t I_b(t)dt \qquad \text{(III. 28)}$$

- Then, we define the theoretical open circuit voltage (OCV-ref) which is calculated using a polynomial function and the open circuit voltage derived by RLS (OCV-actual) ,we deduce the following error;
- Calculation of the estimation error e(k) by equation:

$$e(t) = V_{OC_{ref}}(t) - V_{OC_{acteul}}(t) \quad \text{(III. 29)}$$

- Applying the Adaptive Law **:**The parameter adjustment law is applied based on the computed error.

$$\Delta_{SOC}(t) = \alpha_1 \times V_{OC_{CC}} + \alpha_2 \times V_{OC_{ref}} \quad \text{(III. 30)}$$

$$\dot{\alpha_1} = -\Gamma \times e(t) \times V_{OC_{CC}}(t) \quad \text{(III. 31)}$$

$$\dot{\alpha_2} = -\Gamma \times e(t) \times V_{OC_{ref}}(t) \quad \text{(III. 32)}$$

Δ(t) : Correction parameter.

Γ : Adaptation gain (positive constant).

- In this simulation we used an adaptation gain $\Gamma = 0.0011$
- Final SOC Estimation Correction The output from the Coulomb Counting (CC) method is corrected by adding the adaptive gain .

$$\Delta_{SOC}(t) + SOC_{CC}(t) = SOC_{\text{corrected}}(t) \quad \text{(III. 33)}$$

$SOC_{\text{corrected}}(t)$: corrected estimate of the State of Charge (SOC).

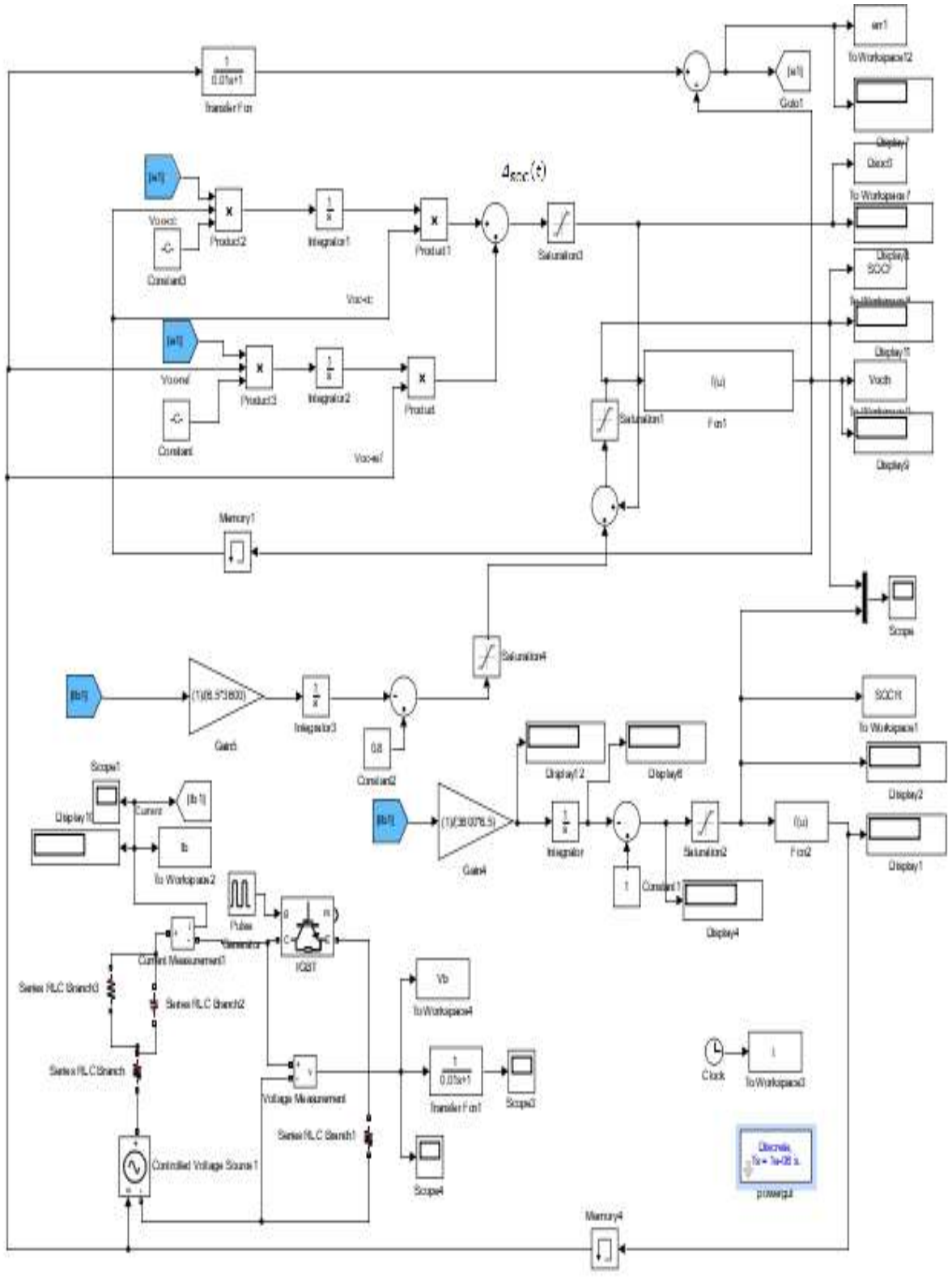

Figure 3-10 :Matlab/Simulink diagram for battery and Proposition of an adaptive law to correct the Coulomb Counting (CC) method

The schematic diagram shown in the previous figure from Matlab/Simulink represents a hybrid battery model designed to correct the estimation of the State of Charge **(SOC)** using the Coulomb Counting **(CC)** method, integrated with Model Reference Adaptive Control (**MRAC**) and the Recursive Least Squares **(RLS)** algorithm through a structured process.

Initially, a preliminary **SOC** estimate is calculated using the Coulomb Counting method by integrating the current flowing through the battery. However, this estimate may be affected by errors due to inaccurate initial values and noise in current measurements. To address these issues, a reference model representing the ideal **SOC** behavior is used, where the system's initial estimate is compared with the output of this model to compute the estimation error.

The **MRAC** applies an adaptive law to dynamically adjust the correction parameters in order to minimize this error and improve estimation accuracy.

At the same time, the **RLS** algorithm is used to continuously update the battery model parameters based on the available data, contributing to enhanced stability and reliability of the **SOC** estimation under varying operating conditions.

This integration of **MRAC** and **RLS** ensures improved SOC estimation performance compared to traditional methods that rely solely on Coulomb Counting.

3.3.3.1 Results of the Proposed SOC Estimation Method :

The proposed State of Charge (SOC) estimation method, based on the Coulomb Counting (CC) technique enhanced by integrating the Recursive Least Squares (RLS) algorithm and the Model Reference Adaptive Control (**MRAC**) unit, was evaluated using three incorrect initial SOC values and three correct reference values.

- **In the first simulation :** the following values were set: **SOC_actual = 100%** and **SOC_initial = 80%**, As shown in Figure 3-11, the estimated SOC (SOC_esti) using the proposed method (CC with MRAC) quickly rises and converges with the actual SOC (SOC_actual) within approximately 40 seconds, represented by the red dashed line. Afterwards, SOC_esti remains relatively stable. The estimation error using this method was **0.0188%**, calculated using the **Mean Absolute Error (MAE)**. In contrast, the SOC estimation using only the Coulomb Counting method (SOC_ini(CC)), shown in yellow

in Figure 3-11, never approached the actual SOC value (SOC_actual), with an average estimation error of approximately **20%**.

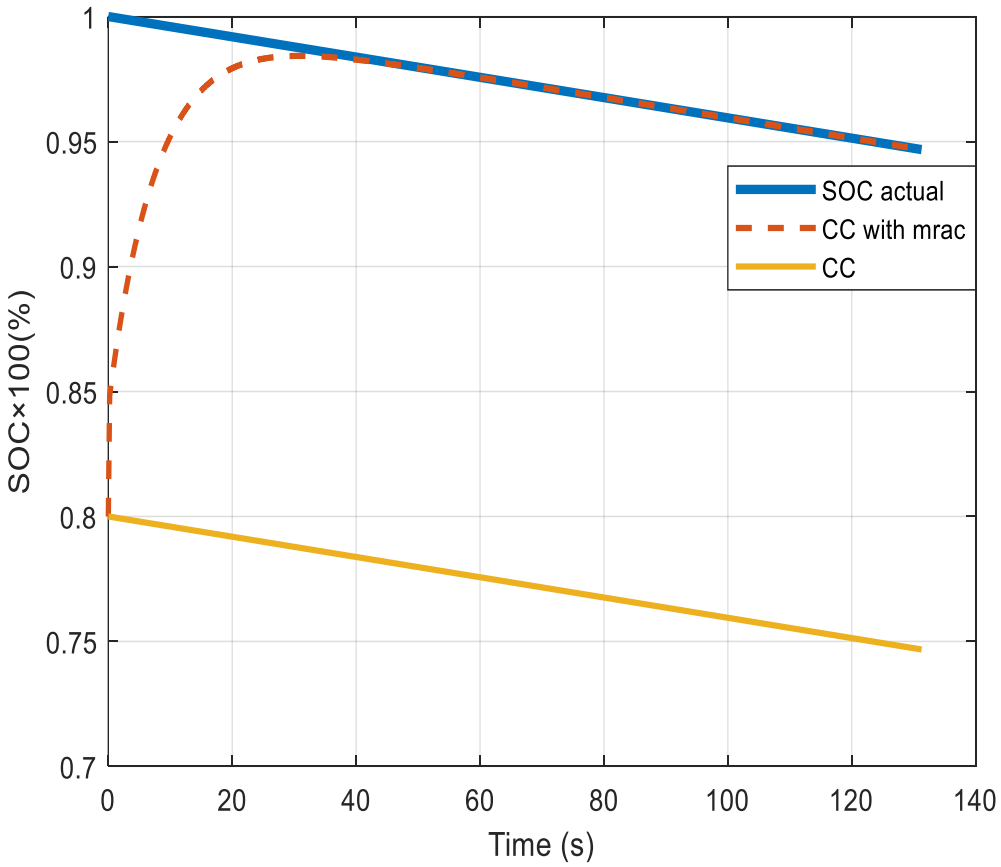

Figure 3-11 : Results of the first experiment

- **In the second simulation :**, the values were set as follows: **SOC_actual = 80%** and **SOC_initial = 100%** , As shown in Figure 3-12, the estimated SOC (SOC_esti) using the proposed method (CC with MRAC) decreases quickly and converges with the actual SOC within approximately 50 seconds, represented by the red dashed line. Afterwards, SOC_esti remains relatively stable. The estimation error using this method was **0.0273%**, calculated using the **MAE**. In contrast, the SOC estimation using only the Coulomb Counting method (SOC_ini(CC)), shown in yellow in Figure 3-12, never approached the actual SOC value (SOC_actual), with an average estimation error of approximately **20%**.

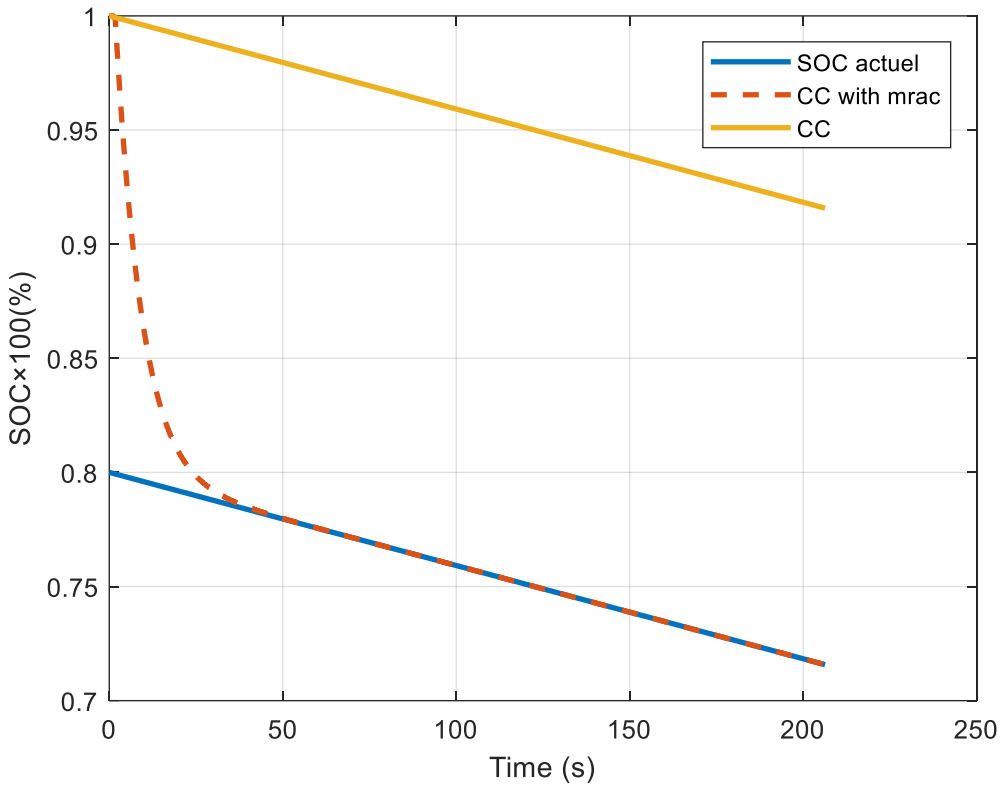

Figure 3-12 : Results of the second experiment

- **In the third simulation :** the values were set as follows: **SOC_actual = 60%** and **SOC_initial = 80%**, As shown in Figure 3-13, there is a very slight increase in the SOC_esti curve up to about **85%** in 1 second, after which the estimated SOC (CC with MRAC) rapidly decreases and converges with the actual SOC (SOC_actual) within approximately 40 seconds, represented by the red dashed line. Afterwards, SOC_esti remains relatively stable. The estimation error using this method was **0.026%**, calculated using the **MAE**. In contrast, the SOC estimation using only the Coulomb Counting method (SOC_ini(CC)), shown in yellow in Figure 3-13, never approached the actual SOC value (SOC_actual), with an average estimation error of approximately **20%**.

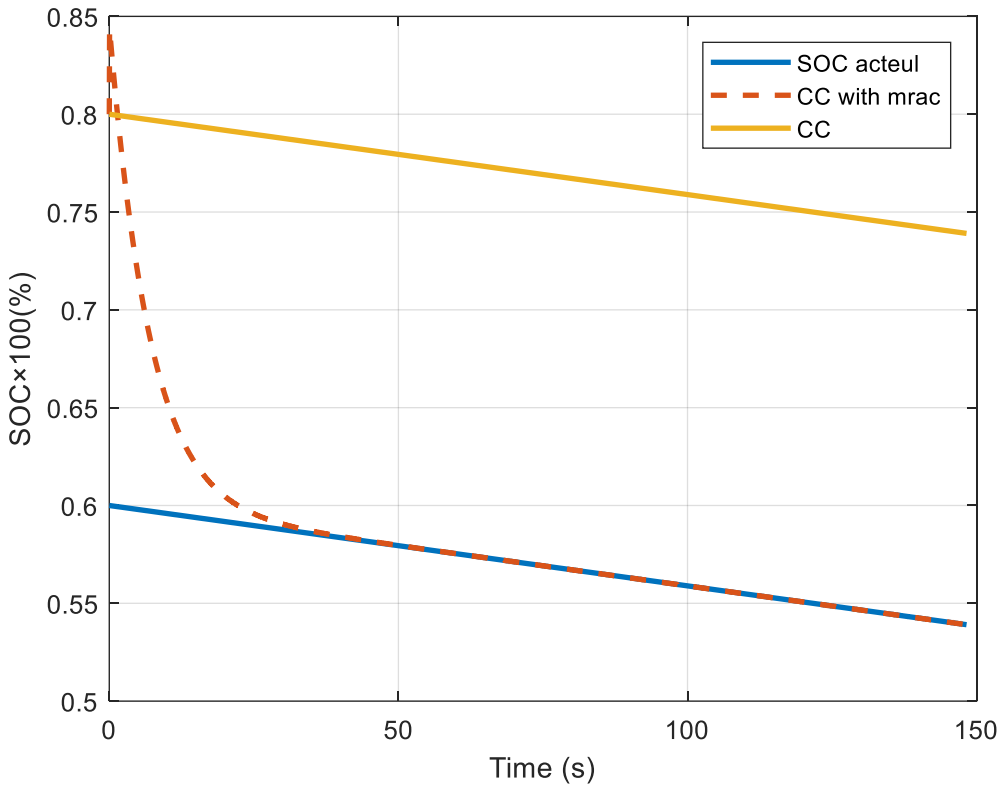

Figure 3-13 : Results of the third experiment

✓ MEAN ABSOLUTE ERROR OF SOC ESTIMATION:

SOC Initial Value	SOC actuel Value	SOC Estimation Error (CC Method)	SOC Estimation Error (CC + MRAC)
80%	100%	20%	0.0216%
100%	80%	20%	0.0273%
80%	60%	20%	0.026%

Table 14 :Mean Absolute error of SOC Estimation

To calculate the **Mean Absolute Error (MAE)** , we need to use the abbreviation MAE in the MATLAB window in the following way :

MAE= (abs (SOCacteul – SOCeastim)) (III. 34)

It can be concluded from these results that the proposed State of Charge (SOC) estimation method, which combines the Coulomb Counting (CC) method with the Recursive Least Squares (RLS) algorithm and the Model Reference Adaptive Control (MRAC) unit, is capable of correcting incorrect initial SOC values and reaching the actual SOC within approximately 80 seconds. This allows for accurate determination of the battery's SOC even when the initial value is incorrect.

In contrast, SOC estimation using the CC method alone leads to significant estimation errors, as it never converges to the actual SOC due to the absence of a correction mechanism.

Table 14 shows the SOC estimation error calculated using the Mean Absolute Error (MAE). The average SOC estimation error using the proposed method is:

$$MAE_G = \frac{MAE_1 + MAE_2 + MAE_3}{3} = \frac{0.0216 + 0.0273 + 0.026}{3} \quad \text{(III. 35)}$$

$$MAE_G = 0.0249\% \quad \text{(III. 36)}$$

3.3.4 Kalman filter based SOC estimation:

First, we process the battery model that we will experiment on, and for this purpose, we choose the following Thevenin model.

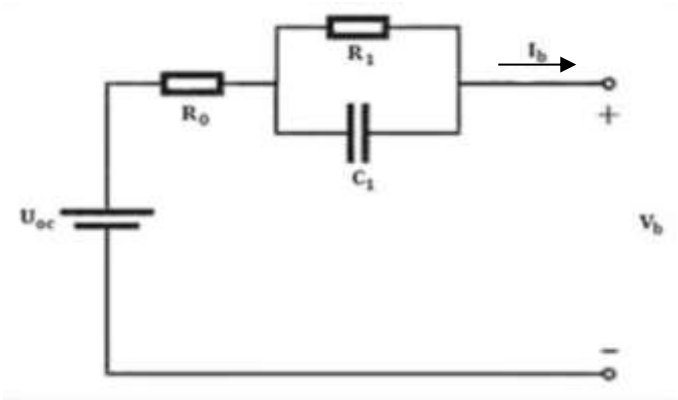

Figure 3-14 :Thevenin model with a polarization branch[21]

The equations of the Thevenin model are:

$$\dot{V}_P = \frac{dV_P}{dt} = \frac{-1}{R_P.C_P} + \frac{1}{C_P}.I_b(t) \quad \text{(III. 37)}$$

$$S\dot{O}C(t) = \frac{dSOC}{dt} = \frac{1}{Cn}.I_b(t) \quad \text{(III. 38)}$$

$$V_b = y(t) = Voc - R_s.I_b - V_P \quad \text{(III. 39)}$$

Since the relationship between open-circuit voltage (OCV) and state of charge (SoC) in lithium-ion batteries is only piecewise linear in practical applications, the voltage across the main (bulk) capacitor in the model can be expressed as follows:

$$Voc(t) = l_1.SOC(t) + l_2 \quad \text{(III. 40)}$$

$$y(t) = V_b = l_1 SOC + l_2 - R_s.I_b - V_P + w(t) \quad \text{(III. 41)}$$

$$y(t) = V_b - l_2 \quad \text{(III. 42)}$$

When the system's state equation is nonlinear, the standard Kalman filter cannot be applied directly. In such cases, the system must first be linearized using a Taylor series expansion around the current state estimate. The resulting approach, which handles nonlinear models through this linearization process, is known as the Extended Kalman Filter (EKF).

$$X = \begin{bmatrix} x_1 \\ x_2 \end{bmatrix} \qquad x_2 = SOC \qquad x_1 = V_P \quad \text{(III. 43)}$$

$$y(t) = V_b \qquad u = I_b \quad \text{(III. 44)}$$

If the system input of a model is defined as u(t) = I and the output is defined as y(t) = Vo, then the battery model can be written as:

$$\begin{cases} \dot{X}(t) = A.X + B.U + v(t) \\ Y(t) = C.X + D.U + w(t) \end{cases} \quad \text{(III. 45)}$$

W(t): system noise.

V(t): measurement noise .

Where : We substitute the values:

$$v(t) = \begin{bmatrix} 10^{-6} & 0 \\ 0 & 10^{-5} \end{bmatrix} \qquad w(t) = 0.01 \qquad \text{(III. 46)}$$

$$\begin{cases} A = \begin{bmatrix} \frac{-1}{R_P C_P} & 0 \\ 0 & 0 \end{bmatrix} \\ B = \begin{bmatrix} \frac{1}{C_P} \\ \frac{1}{C_n} \end{bmatrix} \\ C = [-1 \quad l_1] \\ D = R_s \end{cases} \qquad \text{(III. 47)}$$

state update equation

$$\hat{\dot{X}} = A.\hat{X} + B.U + K(y - C.\hat{X}) \qquad \text{(III. 48)}$$

- The term $A.\hat{X} + B.U$ represents the state prediction.
- The term $K(y - C.\hat{X})$ represents the correction of the estimate based on the difference between the actual and predicted measurements.
- The term $(y - C.\hat{X})$ represents the **measurement innovation** or **innovation term**.
- K is the Kalman gain.

The Kalman gain is computed at each iteration based on the predicted errors and the levels of uncertainty (noise) in both the states and the measurements.

The dynamic behavior of the filter relies on the initialization of the process noise matrix **Q**, the measurement noise matrix **R**,and the error covariance matrix **P.**

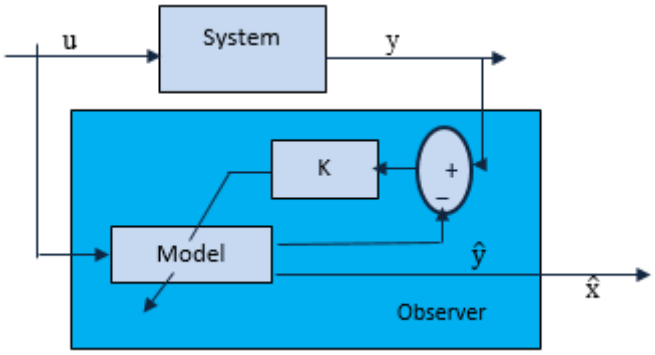

Figure 3-15 :Principle block diagram of the Kalman filter [16]

To implement the optimal observer as shown in Figure 3-15, the Kalman filter algorithm is divided into two main parts as follows :

- ✓ Predict the system state, output, and estimation error
- ✓ Correct and update the current state estimate based on the system output measurement

This process occurs in two phases during each sampling interval, as shown in Figure 3-16 :

1. The prediction phase, where the current state, expected output, and error covariance are estimated .
2. The correction phase, where the actual system output measurement is used to adjust and update the state estimate and error covariance .

The core of the Extended Kalman Filter (**EKF**) is to compare the predicted value with the actual measurement, and then adjust the Kalman gain accordingly .

The larger the error, the greater the gain, leading to a bigger correction of the estimate. Conversely, when the error is small, the gain is reduced, and the correction is less significant .

Therefore, the **EKF** algorithm is applied to accurately estimate the State of Charge (**SOC**) of a lithium-ion battery pack. [16]

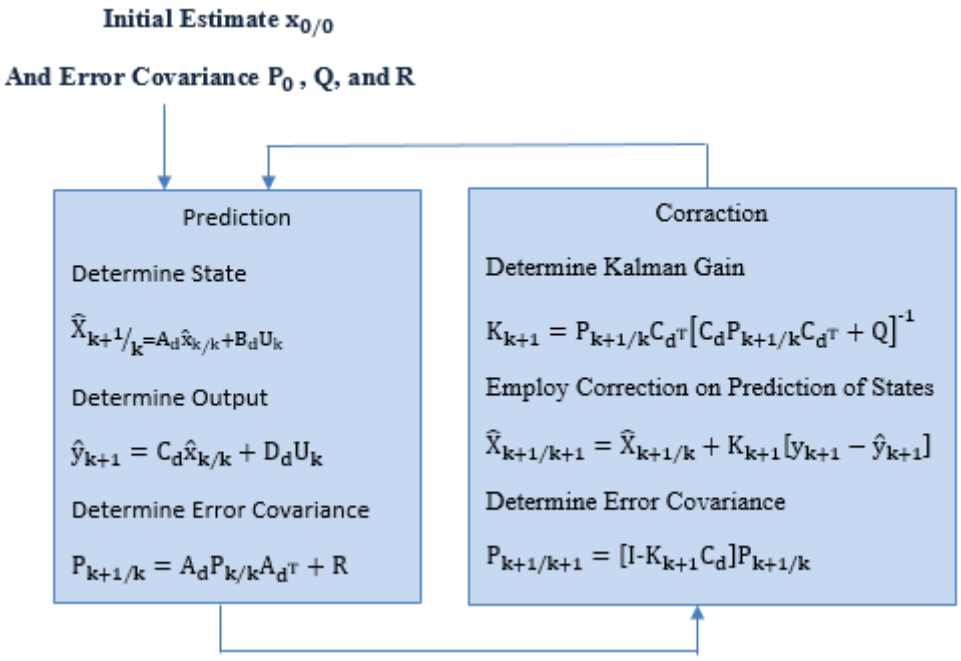

Figure 3-16: Computation steps of the EKF algorithm.[16]

3.3.4.1 Result of Simulation:

To represent the discharge state of a lithium-ion battery under normal usage conditions and to verify the effectiveness of the State of Charge (SOC) estimation method, a series of discharge were conducted. At normal temperature, the battery was discharged starting from an open-circuit voltage (OCV) of 3.382 V (corresponding to 100% SOC) using a constant discharge current, until the OCV reached 3.368 V (corresponding to 88% SOC), see figure 3-17.

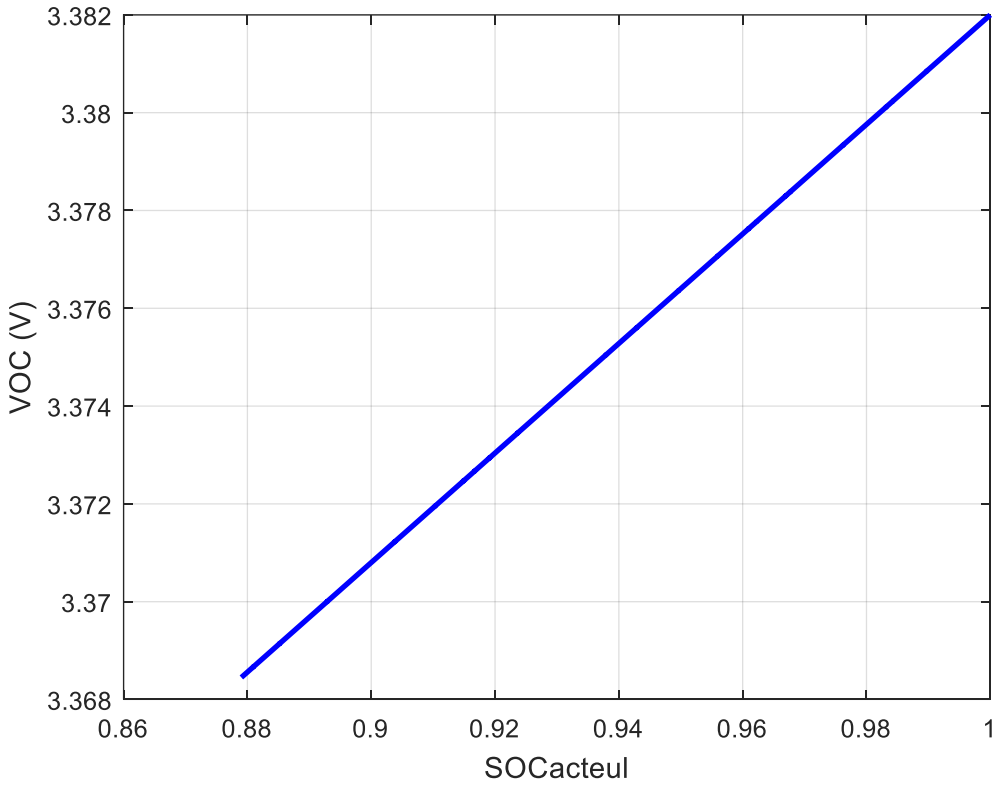

Figure 3-17 :OCV-SOC curve

The simulation is evaluated by comparing the estimated SOC by KF that implements by Matlab simulink and SOC proposed. The SOC estimation accurately evaluates the absolute value by subtracting the true SOC from the estimated SOC in percentage. The time transition of the estimated SOC and reference SOC is shown in Fig.3-18. The average error for the SOC estimation experiment is 0%. The simulation results show that the proposed KF-based SOC

estimation method is effective and can estimate the battery SOC accurately.

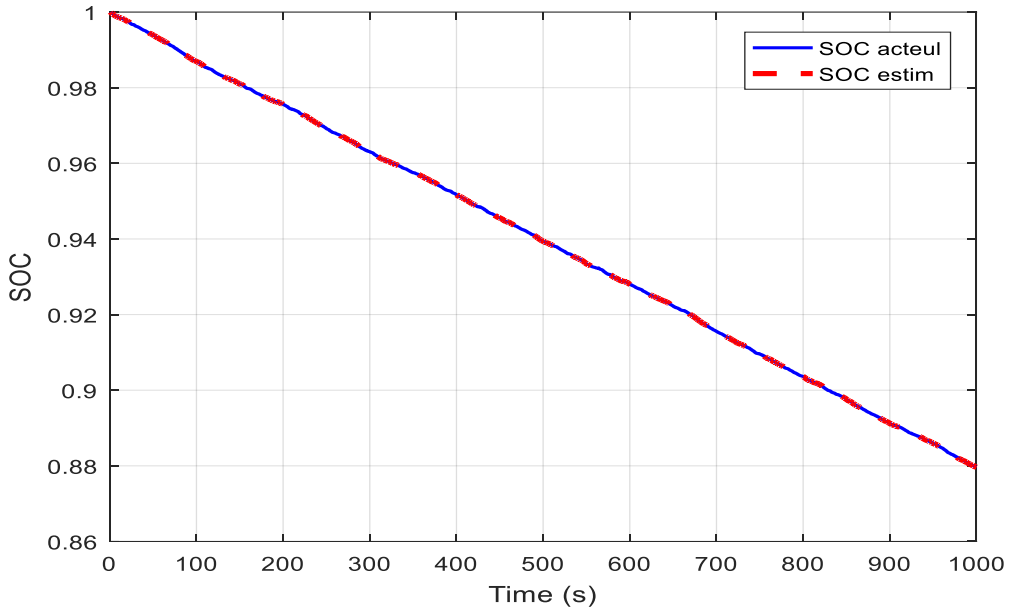

Figure 3-18: SOC estimation results

The estimation accuracy was calculated based on the absolute difference between the measured battery voltage Vb and the estimated voltage, the measured voltage Vb meas was obtained experimentally.

Figure 3-19 illustrates the time-based variation of both the estimated battery voltage Vb estim and the reference measured voltage Vb meas during the discharge process.

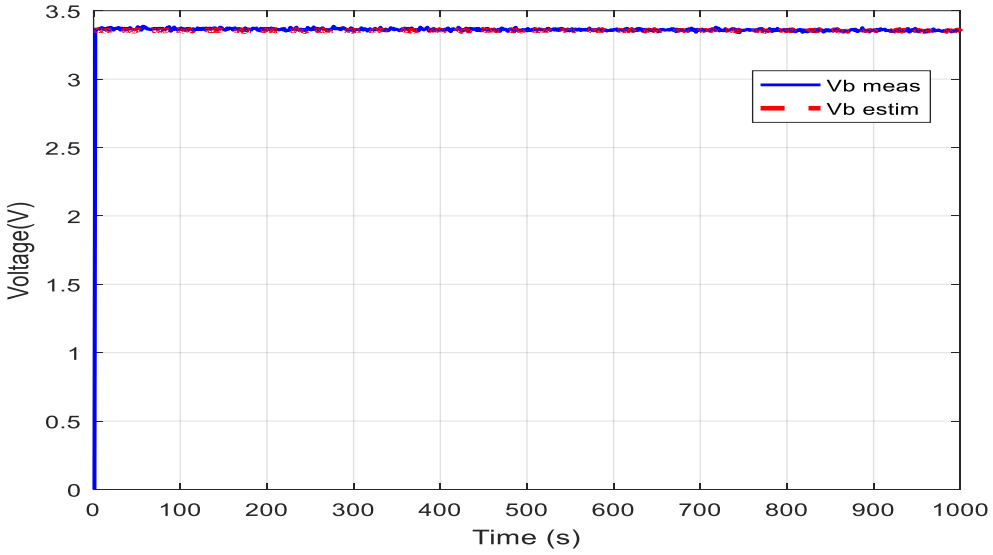

Figure 3-19 :Vb estimation results

The estimation results by KF showed that the estimated SOC values closely match the reference values calculated through integration, indicating that the Kalman Filter (KF)

algorithm is capable of providing accurate SOC estimation during the discharge process.

(To view the programme used in this simulation look the Appendix).

- **Comparison Between the Studied Methods:**

Method	Accuracy	Computational Complexity	Adaptability	Noise Handling	Response Time	Advantages
RLS Only	Medium	Medium	Medium	Medium	Medium	Improved estimation over Coulomb Counting
Coulomb Counting	Low to Medium	Low	Weak	Weak	Fast	Simple and easy to implement
Coulomb + MRAC + RLS	Medium to High	Medium	Good	Good	Medium to Fast	Reduces accumulated errors, adapts to battery state changes
Extended Kalman Filter (EKF)	High	High	High	High	Fast and Adaptive	High accuracy, robust to noise and nonlinearities

Table 15 : Comparison Between the Studied Methods

3.4 Conclusion:

In this chapter, three important methods are proposed to estimate the state of charge (SOC) of the battery have been tested and compared, Each the method has demonstrated its effectiveness and its capacity, in particular under variable operating conditions that affect the accuracy of the COS estimation. This answers the second question asked in the general introduction. This chapter provides a basis for understanding the COS estimation mechanisms, helping to improve the reliability of the energy management system and improving the performance of the battery under various operating conditions.

General Conclusion

General Conclusion:

The accurate estimation of the State of Charge (SoC) is critical for optimizing the performance, safety, and longevity of battery systems, particularly in renewable energy applications like solar power storage and electric vehicles. Various methods have been developed to quantify SoC, each with its own strengths and limitations. This conclusion summarizes the key characteristics of four widely used techniques: Kalman Filter, Coulomb Counting, Coulomb Counting Combined with Recursive Least Square and MRAC Controller and RLS Method .

As a result, a set of conclusions has been deduced.:

Accuracy: The Kalman filter and Coulomb Counting Combined with Recursive Least Square and MRAC Controller are the most accurate methods, because they integrate dynamic correction mechanisms. Coulomb counting alone is less accurate due to time drift. **Computational Complexity**: Coulomb counting is the simplest, while the methods based on the Kalman filter and Coulomb Counting Combined with Recursive Least Square and MRAC Controller require higher computing power.

Adaptability: Coulomb Counting Combined with RLS and MRAC Controller -based methods excel in adapting to changing battery conditions, which makes them suitable for long-term use. Real-time

Applicability: Kalman filter and Coulomb Counting Combined with RLS and MRAC Controller -based methods are ideal for real-time applications, while Coulomb counting alone may require frequent recalibration.

For this purpose, for high-precision applications such as electric vehicles and renewable energy systems, advanced methods such as the Kalman filter or Coulomb counting with RLS and MRAC are preferred because of their ability to provide a reliable and adaptive estimate of the SOC. Simpler methods such as Coulomb counting remain useful for basic applications where calculation efficiency takes precedence over absolute accuracy.

These techniques collectively contribute to the development of robust battery management systems (BMS), guaranteeing safe, efficient and sustainable operation of energy storage systems.

Références

[1] Agus Kustiman and others.(2019), "Battery State of Charge Estimation Based on Coulomb CountingCombined with Recursive Least Square and PI Controller" ,Universitas Gadjah Mada, Indonesia.

[2] **Chen, M., Harb, M., & Rizzoni, G. (2018).** *Advanced nonlinear battery modeling for state estimation and control.* IEEE Transactions on Industrial Electronics, 65(7), 5774-5783.

[3] Spångberg, C. (2022). *State of Health estimation of battery systems* (Master's thesis). Lund University, Sweden; Technical University of Denmark .

[4] «https://www.energy.gov/eere/solar/solar-energy-technologies-office,» [En ligne].

[5] D. L. a. T. B. Reddy, HANDBOOK OF BATTERIES, Third Edition.

[6] M. Boxewll, Solar Electricity Handbook, Green stream publishing, 2012.

[7] Deshpande, 3R.P Ultracapasitors: Future of Energy Storage page 42, 2015.

[8] Bordji Abdelmalek et Flitti Hamza " Etude et simulation des éléments de chargeurs intégrés pour Véhicule électrique" mémoire de master, Université Abdelhamid Ibn Badis Mostaganem, 2019..

[9] chapter 11 BOOK "Fuel Cell Systems Explained".

[10] Y. Gopal, "Storage of Hydrogen Energy," *LinkedIn*. [Online]. Available: https://www.linkedin.com/pulse/storage-hydrogen-energy-yuvaraj-gopal-vtqfc.

[11] A. Harbaoui, Identification Parametrique des Sources a Puissance Finie. MEMOIRE DE MASTER, Universite Mohamed khider de Biskra, 2023-2024.

[12] Dynamic Internal Resistance Modeling and Thermal Characteristics of Lithium-ion Batteries for Electric Vehicles by Considering State of Health.

[13] ResearchGate, [Online]. Available: https://www.researchgate.net.

[14] S. D. S. J. M. Dong Zhang, Lithium-Ion Battery State Estimation for a Single Particle Model with Intercalation-Induced Stress.

[15] H. W. Y. S. Z. W. T. &. H. S. Fang, State of charge estimation for lithium-ion batteries: An adaptive approach. Control Engineering Practice, 25, 45–54., 2014.

[16] D.-W. C. S.-H. Yang, «https://doi.org/10.1051/e3sconf/20185702006 "SOC Estimation of Lithium-Ion Battery Based on Kalman Filter ",» 2018.

[17] K. I.-B. Mondhir, "Commande et Gestion d'énergie d'un système Hybride PV-Batterie ",MÉMOIRE DE MASTER , Université Mohamed Khider de Biskra , 2025.

[18] *"State of Charge Estimation Using Extended Kalman Filters for Battery Management System"* conducted by Carlo Taborelli and Simona Onori, an Extended Kalman Filter (**EKF**) was developed to estimate the SoC of a lithium-ion battery used in electric bicycles

[19] *(By Da-Yan Liu1, Wen Chen2 , Driss Boutat1 . 'State of Charge Estimation of Lithium-ion Batteries based on Fractional-order Modulating Functions'. Proceedings of the 2024 12th International Conference on Systems and Control, Batna, Algeria, November 03-05, 2024*

[20] H. Bia, B. Khadem, and S. Bellili, *Étude des techniques d'estimation de l'état de charge de la batterie d'un système embarqué*, Mémoire de fin d'étude, Master Académique, Université Echahid Hamma Lakhdar d'El-Oued, 2019–2020.

[21] ResearchGate, "*ResearchGate – Find and share research*," [Online]. Available: https://www.researchgate.net.

[22] Epic Power Converters, S.L. (n.d.). *Application Note - AN026: Battery state of charge calculation with EPC converters*. Epic Power Converters, S.L. Retrieved from https://www.epicpower.es

Appendix

Numerical optimization technique:

```
% SOC estimation with a Kalman filter
% Electrical model: RC equivalent circuit (1st order)

clc; clear; close all;

% --------- Battery parameters ---------
%Q = 3600;             % Battery capacity (in Coulombs)
Q = 8280;
Rs = 0.01;            % Series resistance (Ohms)
%Rp = 0.02;            % Polarization resistance (Ohms)
Rp = 0.004;
%Cp = 2000;            % Polarization capacitance (Farads)
Cp = 156;
dt = 1;               % Time step (seconds)
SOC0 = 1.0;           % Initial SOC (State of Charge)

% --------- Simulated input vectors ---------
N = 1000;
I = 1 + 0.5*randn(1, N);  % Current (A)
SOC_true = zeros(1, N);
Vp_true = zeros(1, N);      % Voltage across the RC
V_meas = zeros(1, N);
OCV = @(soc) 3.27 + 0.112*soc;   % Linear OCV model for demonstration
%OCV = @(soc) 3 + 0.7*soc;
SOC_true(1) = SOC0;
Vp_true(1) = 0;
for k = 2:N
    % SOC evolution (Coulomb counting model)
    SOC_true(k) = SOC_true(k-1) - dt*I(k-1)/Q;
    % Voltage evolution across the RC
    dVp = (-Vp_true(k-1)/(Rp*Cp) + I(k-1)/Cp)*dt;
    Vp_true(k) = Vp_true(k-1) + dVp;
    % Measured voltage
    V_meas(k) = OCV(SOC_true(k)) - Vp_true(k) - Rs*I(k);
end

% --------- Kalman Filter ---------
X_est = zeros(2, N);    % [SOC ; Vp]
X_est(:,1) = [SOC0; 0];
P = eye(2)*1e-4;          % Initial covariance matrix
Qn = diag([1e-6, 1e-5]); % Process noise
R = 0.01;                 % Measurement noise
for k = 2:N
    % --- State model ---
    A = [1, 0; 0, 1 - dt/(Rp*Cp)];
    B = [-dt/Q; dt/Cp];
    C = [OCV_deriv(X_est(1,k-1)), -1];
    D = -Rs;

    % --- Prediction ---
    X_pred = A * X_est(:,k-1) + B * I(k-1);
    P_pred = A * P * A' + Qn;
    % --- Update ---
    y_pred = OCV(X_pred(1)) - X_pred(2) - Rs * I(k);
    H = C;
    K = P_pred * H' / (H * P_pred * H' + R);
    X_est(:,k) = X_pred + K * (V_meas(k) - y_pred);
    P = (eye(2) - K * H) * P_pred;
```

```
end

% --------- Plotting ---------
t = 1:N;
figure;
plot(t, SOC_true, 'k', 'LineWidth', 1.5); hold on;
plot(t, X_est(1,:), 'r--', 'LineWidth', 1.5);
xlabel('Time (s)'); ylabel('SOC');
legend('True SOC', 'Estimated SOC');
title('SOC Estimation with Kalman Filter and RC Model');
grid on;

% --------- Approximate derivative of OCV ---------
function d = OCV_deriv(soc)
    % Simple approximation (constant)
    d = 0.7;  % For the model OCV = 3 + 0.7*soc
end
```